EBioMedicine 44 (2019) 582–596

Contents lists available at ScienceDirect

EBioMedicine

journal homepage: www.ebiomedicine.com

EBioMedicine
Published by THE LANCET

Activation of arcuate nucleus GABA neurons promotes luteinizing hormone secretion and reproductive dysfunction: Implications for polycystic ovary syndrome

Mauro S.B. Silva [1], Elodie Desroziers [1], Sabine Hessler, Melanie Prescott, Chris Coyle, Allan E. Herbison, Rebecca E. Campbell *

Centre for Neuroendocrinology and Department of Physiology, School of Biomedical Sciences, University of Otago, Dunedin 9054, New Zealand

ARTICLE INFO

Article history:
Received 15 March 2019
Received in revised form 26 May 2019
Accepted 30 May 2019
Available online 6 June 2019

Keywords:
GnRH neurons
Luteinizing hormone
Mouse
Optogenetics
Chemogenetics
PCOS

ABSTRACT

Background: Enhanced GABA activity in the brain and a hyperactive hypothalamic-pituitary-gonadal axis are associated with polycystic ovary syndrome (PCOS), the most common form of anovulatory infertility. Women with PCOS exhibit elevated cerebrospinal fluid GABA levels and preclinical models of PCOS exhibit increased GABAergic input to GnRH neurons, the central regulators of reproduction. The arcuate nucleus (ARN) is postulated as the anatomical origin of elevated GABAergic innervation; however, the functional role of this circuit is undefined.

Methods: We employed a combination of targeted optogenetic and chemogenetic approaches to assess the impact of acute and chronic ARN GABA neuron activation. Selective acute activation of ARN GABA neurons and their fiber projections was coupled with serial blood sampling for luteinizing hormone secretion in anesthetized male, female and prenatally androgenised (PNA) mice modelling PCOS. In addition, GnRH neuron responses to ARN GABA fiber stimulation were recorded in *ex vivo* brain slices. Chronic activation of ARN GABA neurons in healthy female mice was coupled with reproductive phenotyping for PCOS-like features.

Findings: Acute stimulation of ARN GABA fibers adjacent to GnRH neurons resulted in a significant and long-lasting increase in LH secretion in male and female mice. The amplitude of this response was blunted in PNA mice, which also exhibited a blunted LH response to GnRH administration. Infrequent and variable $GABA_A$-dependent changes in GnRH neuron firing were observed in brain slices. Chronic activation of ARN GABA neurons in healthy females impaired estrous cyclicity, decreased corpora lutea number and increased circulating testosterone levels.

Interpretation: ARN GABA neurons can stimulate the hypothalamic-pituitary axis and chronic activation of ARN GABA neurons can mimic the reproductive deficits of PCOS in healthy females. Unexpectedly blunted HPG axis responses in PNA mice may reflect a history of high frequency GnRH/LH secretion and reduced LH stores, but also raise questions about impaired function within the ARN GABA population and the involvement of other circuits.

1. Introduction

Mammalian fertility is dependent upon the appropriate function of the gonadotropin-releasing hormone (GnRH) neuronal network in the brain. GnRH neurons, the final output neuron of this network, secrete pulses of GnRH peptide into the pituitary portal system to drive the pulsatile release of the gonadotropin hormones luteinizing hormone (LH) and follicle-stimulating hormone from the pituitary gland [1,2]. Circulating gonadal steroid hormone levels and a variety of other cues about the internal and external environment must be appropriately conveyed to GnRH neurons for proper reproductive function. This occurs largely through an upstream afferent, steroid hormone-sensitive neuronal network [3,4]. However, our understanding of the identity, relative contribution and significance of individual neuronal components in this connectome remains incomplete.

Dysfunction within the GnRH neuronal network is known to result in infertility. Polycystic ovary syndrome (PCOS), the most prevalent endocrine disorder leading to female infertility worldwide [5,6], is

* Corresponding author at: Centre for Neuroendocrinology & Department of Physiology, School of Biomedical Sciences, University of Otago, 270 Great King Street, Dunedin 9054, New Zealand.
E-mail address: rebecca.campbell@otago.ac.nz (R.E. Campbell).
[1] equal contribution.

https://doi.org/10.1016/j.ebiom.2019.05.065

Research in context

Evidence before this study

Evidence to date suggests that enhanced GABA levels, GABAergic drive and GABAergic innervation to GnRH neurons are associated with the neuroendocrine and reproductive impairments of PCOS. Anatomical evidence in a pre-clinical model of PCOS highlighted GABA neurons originating specifically in the ARN as potential mediators of reproductive axis hyperactivity associated with PCOS features.

Added value of this study

To our knowledge, this is the first study to investigate the functional role of ARN GABA neurons on the reproductive axis. Our findings demonstrate that acute stimulation of ARN GABA neurons can drive increased LH secretion and that chronic ARN GABA activation can recapitulate some of the cardinal features of PCOS. These data support a neuronal mechanism by which the reproductive and neuroendocrine pathology of PCOS could develop. However, variable responses in GnRH neurons and a blunted LH response in mice modelling PCOS, suggest that increased ARN GABA innervation to GnRH neurons may not be the only specific mechanism explaining HPG axis hyperactivity of PCOS.

Implications of all the available evidence

Increased ARN GABA activity is sufficient to stimulate the reproductive axis and drive PCOS-like reproductive dysfunction.

associated with impaired steroid hormone negative feedback [7–9] and a hyperactive GnRH/LH system [6,10,11]. This hyperactive system drives excess androgen production in ovarian theca cells [12,13] and the hyperandrogenism that is a hallmark of PCOS. While oral contraceptive administration can reduce hyperandrogenism, it is not as effective at suppressing LH secretion, suggesting an intrinsic inability or resistance of GnRH neurons to respond to ovarian steroid hormone negative feedback [7–9]. Work by our group and others are highlighting impaired central mechanisms in the neuronal network that regulates GnRH neuron activity that may underpin the neuroendocrine pathophysiology of PCOS [7,14–17].

Clinical and pre-clinical evidence suggest that enhanced GABA levels [18], GABAergic drive [19,20] and innervation [15,21] are associated with the neuroendocrine and reproductive impairments in PCOS. Although GABA is considered the primary inhibitory neurotransmitter of the adult brain, GnRH neurons can respond with excitation to GABA actions *via* the $GABA_A$ receptor ($GABA_AR$), likely due to a higher intracellular chloride concentration [22,23]. Excitatory GABA actions on GnRH neurons, coupled with elevated central GABA levels in PCOS women [18], strongly suggests that increased GABA signalling is driving a hyperactive GnRH/LH system and could be responsible for the associated downstream consequences of PCOS. Previous work, employing viral-mediated tract-tracing from specific GABA populations [24] in a well-characterised prenatally androgenised model of PCOS [16,20,25,26], discovered a previously unidentified, and extremely robust anatomical circuit between GABA neurons in the arcuate nucleus (ARN) of the hypothalamus and GnRH neurons in the rostral forebrain. ARN GABA neuron projections to GnRH neurons are nearly doubled in PCOS-like mice and exhibit significantly reduced progesterone receptor expression [26], highlighting an anatomical framework for impaired steroid hormone feedback [27] and excess excitatory input.

We therefore aimed to investigate the hypothesis that ARN GABA neurons are a functional component of the GnRH neuronal network in both males and females and that altered ARN GABA neuron inputs to GnRH neurons contribute to the neuroendocrine dysfunction of PCOS. To dissect the functional role of ARN GABA neurons modulating LH secretion *in vivo*, we used viral-based Cre-inducible expression of a blue light-sensitive channelrhodopsin-2 accelerated (ChETA) variant [28] in both fertile males and females and in prenatally androgenised (PNA) PCOS-like vesicular GABA transporter (VGAT)-Cre mice. We also applied an *ex vivo* electrophysiological approach to assess the downstream responses in GnRH neurons following the optogenetic activation of ARN GABA neuron projections and the $GABA_AR$-dependency of these responses. Cre-mediated expression of designer receptors exclusively activated by designer drugs (DREADDs) was also employed to assess the impact of both acute and chronic chemogenetic activation of ARN GABA neurons on LH secretion and reproductive function in healthy females.

2. Materials and methods

2.1. Animals

Adult male, female and PNA mice were used for all experiments. Transgenic and wild-type C57BL/6 mice (8–12 weeks) were housed at the Hercus Resource Unit (University of Otago, Dunedin) under 12 h:12 h light-dark cycles (lights on at 0700 h) with *ad libitum* access to water and food. Estrous cyclicity was assessed by daily examination of vaginal cytology in all female mice in order to conduct experiments and collect tissue in the diestrous stage of the cycle. All protocols were approved by the University of Otago Animal Ethics committee (Dunedin, New Zealand).

Homozygous VGAT-Cre (VGAT-$Cre^{+/+}$) mice [24] were crossed with either B6.Cg-Gt(ROSA)26$Sor^{tm9(CAG-tdTomato)Hze}$/J tdTomato floxed-stop reporter mice [29], or ROSA26-CAGS-τGFP floxed-stop reporter mice [30] to generate VGAT-$Cre^{+/-}$;tdTomato and VGAT-$Cre^{+/-}$;τGFP male and female mice respectively to evaluate the efficacy of viral transfection. VGAT-$Cre^{+/-}$;tdTomato mice were crossed with GnRH-GFP mice [31] for *in vitro* studies.

PCOS-like PNA mice were generated as previously described [25]. Briefly, time-mated pregnant dams were injected with 100 μL of dihydrotestosterone (250 μg) in oil, or oil alone to serve as a control, on gestational days 16, 17 and 18. Control vehicle mice ($N = 3$) were grouped with non-treated female mice ($N = 7$) to compose the VGAT-$Cre^{+/-}$ diestrus female group ($N = 10$) as LH release following optogenetic activation was similar among these animals. Female offspring were studied in adulthood.

2.2. Stereotaxic surgery for AAV injections

Adult mice were anesthetized with 2% isoflurane and placed in a stereotaxic apparatus (Stoeling®, Digital Lab Standard) with head and nose fixed. All experiments were performed with sterile instruments and aseptic conditions. Mice were given s.c. injection of carprofen (5 mg/kg) after anesthesia was confirmed. Coordinates according to the mouse brain atlas [32] were −0.9 mm anterior-posterior, ± 0.3 mm medial-lateral and −6.0 mm dorsal-ventral from the dura mater layer and targeting the middle of the rostral-caudal extension of the ARN. Syringes were left *in situ* for 5 min prior to and 10 min following injection. For optogenetic studies, mice received simultaneous bilateral 200 nL injection of either AAV2/9-EF1α-DIO-ChETA-eYFP (3.15×10^{13} GC/mL; PennVector Core) or control virus AAV2/9-EF1α-DIO-eYFP.WPRE.hGH (6.69×10^{13} GC/mL; Penn Vector Core) into the ARN at a rate of 50 nL/min. For chemogenetic activation studies, mice received simultaneous bilateral 100-nL injections of either AAV2/5-hSyn-DiO-hM3D(Gq)-mCherry (5.4×10^{12} GC/mL; UNC Vector Core) or the control virus AAV2/5-hSyn-DiO-mCherry (5.4×10^{12} GC/mL;

UNC Vector Core). Bilateral injections were performed using a custom-made bilateral device bearing two 1 μL Hamilton syringes (#7000) with needles 0.5 mm apart.

2.3. In vitro optogenetic and chemogenetic stimulation and cell-attached recording

Following cervical dislocation and decapitation, 250 μm-thick coronal brain slices containing the rostral preoptic area (rPOA) or ARN were cut with a vibratome (VT1000S; Leica) in an ice-cold solution containing (in mM): NaCl 87, KCl 2.5, $NaHCO_3$ 25, NaH_2PO_4 1.25, $CaCl_2$ 0.5, $MgCl_2$ 6, glucose 25 and sucrose 75. Slices were then incubated at 30 °C for at least one hour in artificial cerebrospinal fluid (aCSF; in mM): NaCl 120, KCl 3, $NaHCO_3$ 26, NaH_2PO_4 1, $CaCl_2$ 2.5, $MgCl_2$ 1.2 and glucose 10. All solutions were equilibrated with 95%O_2/5%CO_2. Loose-seal cell-attached recordings (10–30 MΩ) were made from either ChETA-expressing ARN GABA neurons, hMD3q-expressing ARN GABA neurons, or from GFP-expressing GnRH neurons visualized through an upright microscope fitted for epifluorescence (Olympus, Tokyo, Japan) and constantly perfused with 32 °C warm aCSF. All neurons were first visualized by brief fluorescence illumination (excitation 460–480 nM for GFP and eYFP; excitation 530–560 nM for mCherry) and approached using infrared differential interference contrast optics. Because the ChETA excitation spectrum is similar to that of GFP, recordings did not commence until 10–15 min following fluorescent identification of a GFP-expressing neuron.

Recording electrodes (3.5–5.2 MΩ) were pulled from borosilicate capillaries (Warner Instruments, Hamden, CT) with a horizontal puller (Sutter Instruments, Navato, CA) and filled with aCSF. By applying a slight suction onto the cell membrane of either ChETA-expressing ARN GABA neurons or GFP-positive GnRH neurons, a loose seal was formed and recordings of action current signals were undertaken in the voltage clamp mode with a 0 mV voltage command. Recordings were made from cells held for at least 10–15 min using a Multiclamp 700B amplifier (Molecular Devices, Sunnyvale, CA) connected to a Digidata 1440A digitizer (Molecular Devices). Signals were low-pass filtered at 3 kHz before being digitized at a rate of 10 kHz. Signal acquisition and analysis was carried out with pClamp 10.7 (Molecular Devices). Spikes were detected using the threshold crossing method.

For ChETA activation, blue light was delivered to the slice through a 40× immersion objective (0.8 NA, Olympus) *via* a 470 nm light emitting diode (LED, CoolLED) connected to the vertical illumination port of the microscope. To determine spike fidelity, ARN GABA neurons (expressing mCherry) were patched and blue light (5 ms duration; <1 mW) delivered at 2 or 100 Hz for 5–300 s. Signals were repeated 5–10 times and the average trace was analysed. Spike fidelity was calculated by dividing the number of light-evoked spikes by the number of blue light stimuli and expressed as a percentage with statistical analysis undertaken using Newman-Keuls multiple comparison tests. To assess effects of optogenetic activation on GnRH neurons, cells were recorded for at least 5 min and then 2, 10 and/or 20 Hz blue light given for 5 min. Each cell typically received two different frequency stimulations in random order with only one cell being recorded in each brain slice. The optogenetic activation of transfected ARN GABA fibers was found to generate multiple different effects on rPOA GnRH neurons; these consisted of an immediate but transient excitation (occurring with 1 min of blue light illumination), a delayed excitation (occurring 4.96 ± 0.51 min following blue light) and inhibitory responses. Differences in the percentage of responses displayed by GnRH neurons between the experimental groups were analysed by Chi-square tests.

To assess the effects of CNO on hM3Dq-expressing ARN GABA neurons, cells were recorded for at least 5 min before a 1 μM CNO solution was added to the bath for 2 min. Frequency before and 3–5 min after CNO application was compared and analysed using paired *t*-tests.

2.4. In vivo optogenetic stimulation protocol

Three weeks post-AAV injection, mice were anesthetized with 2% isoflurane and the head and nose were placed and fixed in a stereotaxic apparatus (Stoeling®, Digital Lab Standard). Animals were positioned on a heat-pad and internal body temperature was kept at 35 °C during the whole procedure. A cannula with a 100 μm diameter optical fiber (Thorlabs, Inc.) was implanted into the rPOA using the following mouse brain coordinates: +0.9 to +1.0 mm anterior-posterior, 0.0 mm medial-lateral and −4.2 mm dorsal-ventral [32]. The optical fiber was left *in situ* for at least 30 min before commencing serial blood collection as described below. Serial blood samples (3 μL each) were firstly collected at baseline, −13, −7 and −1 min, considering time 0 as the start of optical stimulation. Blood sample collection was performed every 3 min (at 2, 5, 8, 11, 14 and 17 min from time 0) followed by collection every 6 min until the end of the protocol. The light stimulation consisted of 5 ms blue light (473 nm) pulses using a diode-pumped solid-state (DPSS) laser (IkeCool©) controlled by Grass S88X stimulator. The power light at the tip of the optical fiber was set at 5 mW. Each mouse received photostimulation at 2-Hz and 20-Hz over 10 min, in a random order. Following the light activation protocol, pituitary responsiveness to GnRH was tested by administering GnRH (s.c. 250 μg/kg in 100 nL saline 0.9% solution) and collecting additional blood samples at −5, 0, 5, 10 and 15 min. At the end of the protocol, all mice underwent transcardial perfusion with paraformaldehyde (PFA) 4% and brain tissue was collected for post-mortem examination of transfection and optical probe placement.

3. *In vivo* chemogenetic activation protocols

3.1. Local chemogenetic activation of ARN GABA neurons fibers in the rPOA

As described above for *in vivo* optogenetic stimulation, three weeks post-AAV injection, mice were anesthetized with 2% isoflurane and the head and nose were placed and fixed in a stereotaxic apparatus (Stoeling®, Digital Lab Standard). A Hamilton syringe (1 μL, #7000) containing 400 nL of CNO (30 μM) was implanted into the rPOA using the following mouse brain coordinates: +1.0 mm anterior-posterior, 0.0 mm medial-lateral and −4.2 mm dorsal-ventral [32]. The Hamilton syringe was left *in situ* for at least 20 min before commencing serial blood collection as described below. Serial blood samples (4 μL each) were firstly collected at the baseline: −18, −12, −6 and −3 min considering time 0 as the start of CNO injection at a rate of 50 nL/min. Blood sample collection was performed every 3 min (at 0, 6, 9 and 12 from time 0) followed by collection every 6 min until the end of the protocol. Following the CNO activation protocol, pituitary responsiveness to GnRH was tested by administering GnRH (s.c. 250 μg/kg in 100 μL saline 0.9% solution) and collecting additional blood samples at 78, 84, 90 and 96 min. At the end of the protocol, all mice underwent transcardial perfusion with 4% PFA and brain tissue was collected for post-mortem examination of transfection and optical probe placement.

Chronic chemogenetic activation of ARN GABA neurons: Two weeks post-AAV injection, mice were handled every day to habituate them for serial tail-tip blood sampling for LH secretion and to assess estrous cyclicity. One week after commencing handling, mice were administered drinking bottles with water that was replaced every two days for 2 to 3 weeks. After 2 weeks, mice underwent serial tail-tip blood sampling when in the diestrous stage of the cycle. Briefly, 4 μL blood samples were collected in PBS-Tween from the tail tip every 3–6 min during 2 h between 10:00 h and 14:00 h as previously reported [33]. Blood samples were immediately frozen and keep stored at −20 °C until being processed for the LH by ELISA (described below). CNO was then added to the drinking water (5 mg/kg/mouse/day) and again bottles were replaced every two days for 2 to 3 weeks as described elsewhere [34]. Mice again underwent serial tail-tip blood sampling at the end of the CNO exposure period. Animals were then euthanized by

transcardial perfusion with 4% PFA and brain tissue was collected for post-mortem examination of transfection.

3.2. ELISA for LH and Testosterone levels

A well-established ultrasensitive ELISA was used to measure circulating LH levels [33,35]. Briefly, 96-well high affinity binding plates (Corning®) were coated with a bovine LHβ518B7 monoclonal antibody (1:1000 in PBS; 50 μL per well). Circulating hormone levels were determined using a mouse LH-RP reference provided by Albert F. Parlow (National Hormone & Pituitary Program, Torrance, CA, USA). A rabbit polyclonal primary antibody for LH (1:10,000; rabbit antiserum AFP240580Rb; National Hormone and Peptide Program, USA) and a polyclonal goat anti-rabbit IgG secondary antibody (1:1000; DAKO) were also used for this assay. The sensitivity of this routine LH ELISA assay was 0.002 ng/mL. For optogenetic studies, the average intra-assay coefficient of variation was 3.1% and the inter-assay coefficient of variation was 10.7%. For chemogenetic studies, the average intra-assay coefficient of variation was 2.65% and the inter-assay coefficient of variation was 8.17%.

A commercially available mouse testosterone ELISA kit was used to measure plasma testosterone levels (DEV9911; Demeditec Diagnostics, GmnH) in accordance with manufacturer's instructions. The ELISA sensitivity was 0.066 ng/mL and the intra-assay coefficient of variation for testosterone was 6.97%.

3.3. Ovarian histology and analysis

As previously described [21,25], ovaries were dissected from 4% PFA perfused animals, post fixed overnight at 4 °C, and then stored in 70% ethanol until paraffin embedding. Ovarian sections of 5 μm thickness were collected at 50 μm intervals and stained with hematoxylin and eosin. Sections were visualized with a light microscope (Olympus BX51) and pre-ovulatory follicles and corpora lutea were counted in every section collected throughout each ovary using 10× objective to give overall counts per ovary. Follicle wall composition was determined using the largest preovulatory follicle in each ovary analysed. Images were captured using x20 objectives on an Olympus BX51 light microscope and analysed using ImageJ software (NIH). Total follicle area was measured using the theca-interstitial tissue boundary as the outside extent of the follicle. The area of the follicle was taken at the theca cell-granulosa cell boundary, and finally the area of the antrum was measured, then percentages of the theca cell and granulosa cell compartments of the total follicle area were calculated.

3.4. Free-floating immunohistochemistry

Perfusion fixed brains were saturated in 30% sucrose-Tris buffer saline (TBS) and cut into three or four series of 30-μm thick coronal sections using a freezing stage microtome (Leica®, Wetzlar, Germany). The brain tissue of every experimental animal was subjected to standard single or double immunofluorescent labelling as detailed previously [36] to assess transfection levels and probe or cannula placement.

To determine the proportion of ARN GABA neurons transfected with AAV9-ChETA-eYFP, every third section was labelled with a polyclonal chicken anti-GFP primary antibody (1:2500, Aves Labs Inc.) and an AlexaFluor488 goat anti-chicken secondary antibody (1:200) to detect eYFP transfection. VGAT reporter expression of tdTomato was visualized by its endogenous fluorescent signal. To qualitatively evaluate AAV9-ChETA-eYFP-expressing ARN GABA neuron fibers adjacent to GnRH neurons in the rPOA and assess optical fiber placement, every third section was incubated with polyclonal chicken anti-GFP (1:2500, Aves Labs Inc.) and polyclonal rabbit anti-GnRH (1:5000, gift from Alain Caraty) primary antibodies and subsequently with AlexaFluor488 goat anti-chicken (1:200) and AlexaFluor647 Cy5 donkey (1:500, Abcam®) secondary antibodies.

To quantify the number of AAV5-hM3Dq-mCherry positive cells in the ARN nucleus of VGAT-Cre$^{+/-}$;τGFP mice and determine the specificity of transfection, every fourth section was incubated with polyclonal chicken anti-GFP (1:10,000, Aves Labs Inc.) and polyclonal rabbit anti-mCherry (1:10,000, Abcam) primary antibodies and subsequently with donkey anti-chicken A488 (1:1000, Jackson Immunoresearch Laboratory) and donkey anti-rabbit rhodamine (1:1000, Jackson Immunoresearch Laboratory) secondary antibodies. To qualitatively evaluate AAV5-hM3Dq-mCherry-positive ARN GABA neuron fibers adjacent to GnRH neurons in the rPOA and assess cannula placement, every fourth section was incubated with polyclonal rabbit anti-GnRH (1:5000, gift from Dr. Greg Anderson, University of Otago) and polyclonal rabbit anti-mCherry (1:10,000, Abcam) primary antibodies and subsequently with donkey anti-rabbit rhodamine (1:1000, Jackson Immunoresearch Laboratory) and donkey anti-guinea pig A647 (1:1000, Jackson Immunoresearch Laboratory) secondary antibodies.

All labelled sections were mounted onto glass slides, coverslipped with Fluromount G medium (Sigma-Aldrich, St Louis, MO, USA) and stored at 4 °C until analysis. Primary antibody omission served as a negative control in all procedures.

3.5. Image acquisition and analysis

All brain sections were imaged under an epifluorescence Olympus BX-20 microscope for qualitative assessments and a Nikon A1R Multiphoton confocal microscope with 488, 543 and 647 nm diode lasers for quantitative assessment. To assess ChETA transfection, two representative coronal sections from both the tARN and cARN were selected to image with a Plan NeoFluor 20× objective at 1-μm steps and count single and double labelled tdTomato and eYFP labelled cells in male ($N = 4$) and female ($N = 5$) VGAT-Cre;tdTomato. High magnification and 3D reconstruction images were acquired using a 3× or 5.2× zoom function when suitable and taking *Z*-stacks of 0.5 μm steps using a Plan NeoFluor 40× oil objective (1.30 NA). Confocal images were analysed with NIS-Elements AR 4.00.00 software (Nikon® Instruments Inc.). Animals with off-target injections or optical fiber placement outside the rPOA were excluded from data analysis.

To assess hM3Dq transfection, two representative coronal sections from the rostral, middle and caudal aspects of the ARN were selected to determine the number of mCherry-positive cells in male and female VGAT-Cre;τGFP mice. High magnification images of mCherry-positive fibers adjacent to GnRH neurons were obtained using a Plan NeoFluor 40× oil objective (1.30 NA), 4× zoom function and taking *Z*-stacks of 0.5 μm steps. Confocal images were analysed with NIS-Elements AR 4.00.00 (Nikon® Instruments Inc.) as above.

3.6. Data and statistical analysis

Statistical analysis was performed with PRISM software 7.0 (GraphPad Software, San Diego, CA, USA) and IBM SPSS 24.0 Statistics software (IBM Corp., Armonk, NY, USA). Normal distribution was determined with D'Agostino-Pearson's or Shapiro-Wilk normality test. Statistical analysis of LH values was performed using one-way repeated measures ANOVA with Dunnet's *post hoc* test to compare each point of blood sample collection to the baseline (average of −7- and −1 min). Fold-increase in LH levels was calculated by subtracting the average baseline from the average of the three highest amplitude values of the LH release curve (14, 17 and 23 min) following optogenetic activation as previously reported. Two-way ANOVA with Dunnett's *post hoc* test was applied to confirm that optogenetic-evoked LH secretion was not detected in control groups. To calculate GnRH-evoked LH secretion (pituitary responsiveness test) average baseline values were subtracted from LH peak release at 15 min after s.c. injection of GnRH. Statistical analysis of change in LH and GnRH-evoked LH release used a one-way ANOVA with Tukey's *post hoc* test. Analysis of optogenetic-evoked

spike fidelity in ARN GABA neurons used Kruskal-Wallis H test with Dunn's *post hoc* test.

In chemogenetic studies, the frequency of action potential firing before and after CNO was analysed with a Wilcoxon matched pairs signed rank test. Estrous cycle day frequencies were tested with a multiple Student's *t*-tests and cycle length was compared a Mann-Whitney test. Circulating testosterone levels were analysed by calculating the percentage of change considering water treatment as baseline values and CNO treatment as outcome values, and groups were compared using non-parametric Mann-Whitney *U* test. LH release was analysed with a one-way repeated measures ANOVA and Dunnet's *post hoc* test to compare each point of blood sample collection to the baseline (average of −18, −12, −6 and −3 min). Preovulatory follicle and corpora lutea counts from CNO treated animals were analysed using Students *t*-tests.

In all comparisons, statistical significance was accepted when $p < .05$. Graphical representation to display significant different are shown in figures as * $p < .05$, ** $p < .01$, *** $p < .001$ and **** $p < .0001$.

4. Results

4.1. Selective targeting and activation of ARN GABA neurons with ChETA

VGAT-*ires-cre* mice (VGAT-Cre) [24] were used to conditionally express ChETA, the E123T accelerated variant of channelrhodopsin-2, in ARN GABA neurons. Viral transduction was achieved using a Cre-recombinase-dependent adeno-associated virus serotype 9 (AAV9) vector where ChETA is fused with an enhanced yellow fluorescent protein (eYFP) cassette under the control of an elongation factor 1α (EF1α) promoter (AAV2/9-EF1α-DIO-ChETA-eYFP) [28,37]. To determine the selective targeting and expression of ChETA in ARN GABA neurons, AAV9-ChETA-eYFP was bilaterally injected into the ARN of diestrous female ($N = 5$) and male ($N = 4$) VGAT-Cre;tdTomato reporter mice (Fig. 1*A* and *B*). The expression of AAV9-ChETA-eYFP was largely restricted to the borders of the ARN (Fig. 1 *C-E*) and extensively spread throughout the rostral to caudal extent of the nucleus (Fig. 1*F-H*). The expression of ChETA-eYFP was mainly observed in the cytoplasm and fiber projections of ARN GABA neurons, whereas tdTomato reporter expression was typically found in and around the nucleus of VGAT neurons (Supplementary Fig. 1). Immunohistochemical and confocal analysis revealed that AAV9-ChETA-eYFP was expressed in the vast majority of ARN GABA neurons within the rostral aspect of the ARN of both diestrous female (93.3 ± 1.6%) and male (94.4 ± 1.5%) mice (Supplementary Table 1). Over 80% of GABA neurons in the caudal aspect of the ARN demonstrated ChETA-eYFP expression in both sexes. A very small number of neurons displayed eYFP signal without tdTomato co-expression (~1%) in both sexes, confirming the specificity and Cre-dependence of AAV9-ChETA-eYFP in ARN GABA neurons (Supplementary Table 1).

ChETA-mediated optogenetic activation in neurons enables high spike fidelity, decreased spurious depolarization and faster recovery from post-stimulus inactivation compared to earlier channelrhodopsin variants [28]. To validate the ability of ChETA to elicit faithful light-evoked depolarization of ARN GABA neurons, acute coronal brain slices (250 μm thick) encompassing the ARN were prepared for cell-attached recordings from VGAT-Cre male mice ($N = 6$) that had received bilateral stereotaxic injections of AAV9-ChETA-eYFP into the ARN. All transduced ARN GABA neurons ($n = 19$ cells across six animals) responded to 5 ms blue laser pulses with perfect spike fidelity at 2, 5, 10, 20 and 50 Hz. Spike fidelity was only compromised at 100 Hz when compared to lower frequencies (100 Hz: 72.5 ± 10.0% response rate *vs.* 2–50 Hz: 100.0 ± 0.0%; $p < .001$; Fig. 1*I* and *J*). Frequencies between 2 and 20 Hz were subsequently used to interrogate the role of ARN GABA neurons within the GnRH neuronal network.

4.2. Optogenetic activation of ARN GABA neurons in vivo elicits LH secretion

ARN GABA neurons comprise a heterogeneous population [38] and project to many different areas in the brain including the rostral preoptic area (rPOA) [26], where the majority of GnRH neurons are located in the mouse. ChETA-assisted circuit mapping was employed to probe the biological relevance of ARN GABA neuron projections modulating GnRH/LH release by selectively activating ARN GABA neuronal fibers in the rPOA (Fig. 2*A* and *B*). We hypothesized that optogenetic stimulation of ARN GABA terminals surrounding GnRH neurons would promote GnRH/LH release. To do this, an optical fiber was positioned in the rPOA of VGAT-Cre mice bilaterally transfected with AAV9-ChETA in the ARN. Confocal imaging revealed that GnRH neurons in the rPOA were densely innervated by ChETA-expressing fibers originated from the ARN (Fig. 2*B-G*). *In vivo* optogenetic stimulation of ARN GABA neuronal fibers in the rPOA consisted of 10-min continuous photostimulation (473 nm; 5-ms pulses) delivered at 2 or 20 Hz, in random order for each mouse. As a proxy of GnRH release, circulating LH levels were measured from serial tail-tip blood samples during the optogenetic activation protocol in isoflurane-anesthetized mice, as described previously [39,40]. As mice under isoflurane anesthesia exhibit low circulating LH levels [39,40], observed changes in LH during photostimulation of ChETA-expressing ARN GABA terminals can be attributed to downstream GnRH neuron activation. The evoked LH responses to optogenetic stimulation of ARN kisspeptin neurons, which are known potent regulators of GnRH neurons, is not different between anesthetized and conscious mice [41].

In $Cre^{-/-}$ control diestrous female ($N = 4$) and male ($N = 5$) mice injected with AAV9-ChETA-eYFP, no changes in LH secretion were detected with either 2 or 20 Hz photostimulation (Fig. 2; Supplementary Fig. 2*A,B*). Likewise, photostimulation had no effect on circulating LH levels in control VGAT-Cre diestrous female mice injected with an eYFP control virus (AAV2/9-EF1α-DIO-eYFP, $N = 3$), or in off-target AAV9-ChETA-eYFP transfections of VGAT-$Cre^{+/-}$ male (N = 5) and female (N = 4) mice at any frequency (Supplementary Fig. 2*C,D*).

In VGAT-Cre mice with AAV9-ChETA-eYFP accurately targeted to the ARN, optogenetic activation of ARN GABA terminals at 2 Hz for 10 min did not alter LH levels in males, diestrous females or PNA females. In contrast, 20 Hz photostimulation over 10 min elicited a significant elevation in LH secretion in male, female, and PNA female mice ($p < .05$; Fig. 2*H-M*). The 20 Hz photostimulation of ARN GABA neurons generated a robust increase in LH release in male ($p < .0001$; $F_{13,\ 117} = 8.64$) and diestrous female ($p < .0001$; $F_{13,\ 156} = 4.17$) groups at approximately 8 min following the initiation of photostimulation, and LH levels remained significantly higher than baseline values ($p < .05$) for over 50 min (Fig. 2*N* and *O*). This response was found to be due to photostimulation frequency as opposed to the number of delivered light pulses. Three different photoactivation paradigms were tested in VGAT-Cre diestrous female mice ($N = 3$) injected with AAV9-ChETA-eYFP, including 20 Hz for 10 min, 10 Hz for 10 min, or 10 Hz for 20 min (*i.e.* delivering the same number of light pulses as 20 Hz for 10 min) (Supplementary Fig. 3). As previously observed, 20 Hz activation of ARN GABA neurons promoted robust LH secretion, whereas 10 Hz photoactivation delivered over 10 min or 20 min had no impact on LH levels *in vivo* (Supplementary Fig. 3).

PNA mice also exhibited a significant increase in LH following 20 Hz, but not 2 Hz, photostimulation of ARN GABA fibers in the rPOA ($p < .05$; $F_{13,\ 91} = 6.10$, Fig. 2*J, M* and *P*). However, in contrast to males and diestrous females, PNA females exhibited a delayed rise in LH release, occurring ~11 min following optogenetic activation, that remained elevated for ~18 min and returned to baseline shortly after reaching peak values (Fig. 2*P*). To compare changes in evoked LH, the magnitude of hormone secretion was calculated by averaging LH levels during the 20 Hz optogenetic stimulation at the time points at which peak values were observed, including 17, 23, and 29 min following stimulus initiation. On average PNA mice displayed lower peak LH values than male and

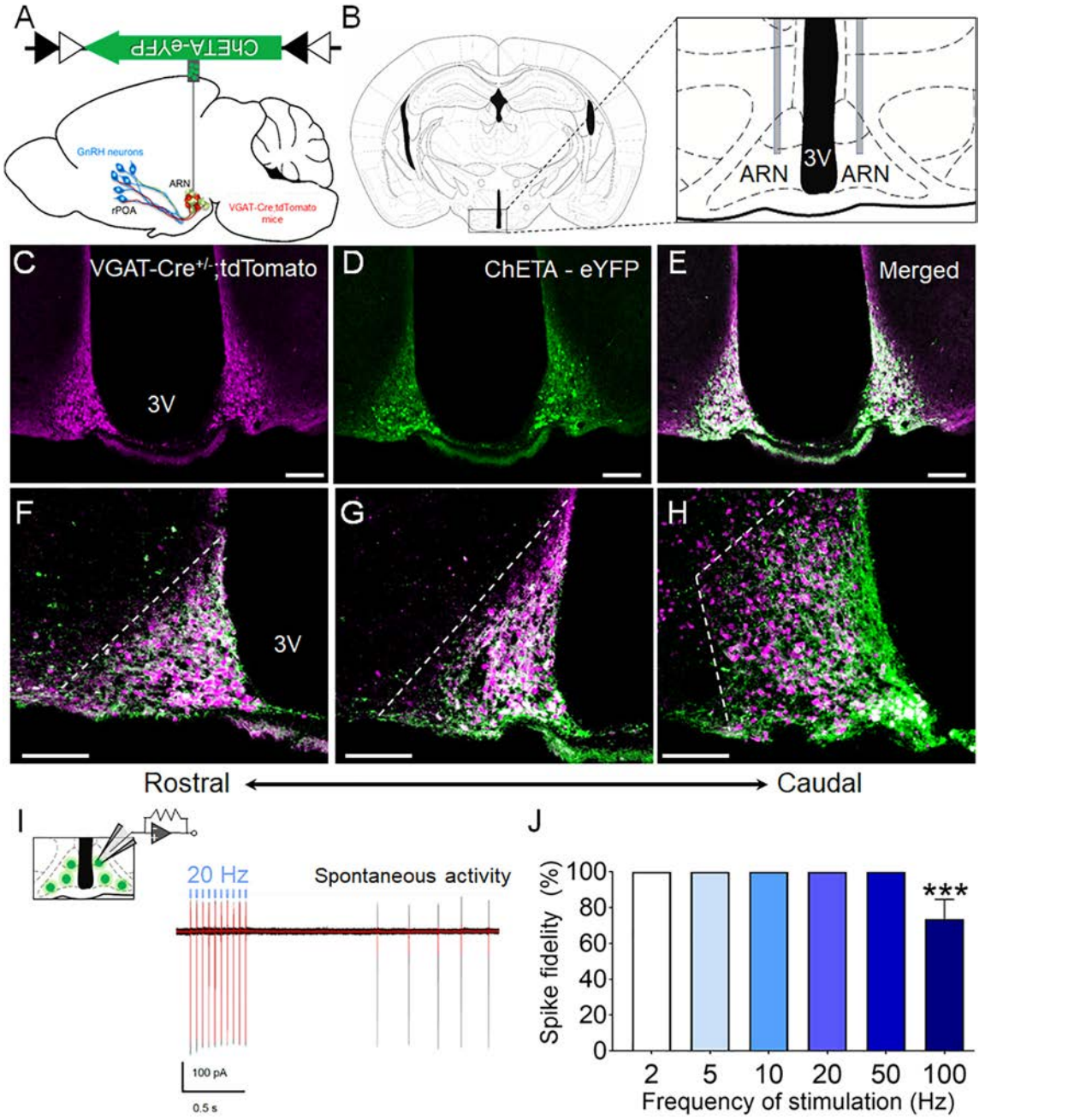

Fig. 1. Selective targeting and activation of ARN GABA neurons with ChETA. (*A,B*) Schematic shows a sagittal and coronal view of the mouse brain, and the ARN location of the bilateral AAV9-ChETA-eYFP injection. (*C-E*) Representative confocal photomicrographs of VGAT-Cre;tdTomato cells in the ARN (*magenta*) transfected with AAV9-ChETA-eYFP (*green*) and their co-localization (*white*). (*F–H*) Representative images of viral transfection from the rostral to caudal extension of the ARN (rARN↔cARN). Dashed white lines delineate the lateral borders of the ARN (3 V = third ventricle; scale bar = 100 μm). (i) Schematic of cell-attached voltage-clamp recordings from ChETA-eYFP-transfected ARN neurons in *ex vivo* brain slices. Representative traces of the 20 Hz optogenetic activation protocol run 5–10 times per cell (*black traces*) and the averaged trace (*red traces*) and spontaneous ARN GABA activity. (*J*) Mean ± SEM evoked spike fidelity at various optogenetic activation frequencies in ARN ChETA-expressing neurons from VGAT-Cre male mice ($N = 6$). ***$p < .001$; Kruskal-Wallis H test with Dunn's *post hoc* test.

female mice (mean peak LH levels: males = 4.94 ± 1.32 ng/mL; diestrous females = 5.18 ± 1.02 ng/mL; diestrous PNA = 2.36 ± 0.50 ng/mL), however, a statistical difference was not found between groups ($p = .21$) when compared using one-way ANOVA with Tukey's *post hoc* test. This was likely influenced by variable baseline LH values between animals and within groups. Therefore, the change in LH release in response to optogenetic activation of ARN GABA neurons (decrement between peak values and average baseline) was also determined (Fig. 3*A*). Absolute change in LH release was significantly lower in PNA mice compared with males and females following 20 Hz optogenetic activation ARN GABA neurons ($p < .05$), whereas no differences between groups were detected when blue light was delivered at 2 Hz (Fig. 3*A*).

Differences in the magnitude of LH responses may arise from differences in the gonadotrope response to GnRH pulses, which display an inverse correlation to the frequency of endogenous GnRH/LH secretion [42]. We hypothesized that long-term elevation of GnRH/LH pulse frequency in PCOS-like PNA mice results in a decreased releasable pool of LH in the pituitary. To test this hypothesis, $Cre^{-/-}$ male, diestrous female and PNA female mice received a single s.c. injection of exogenous

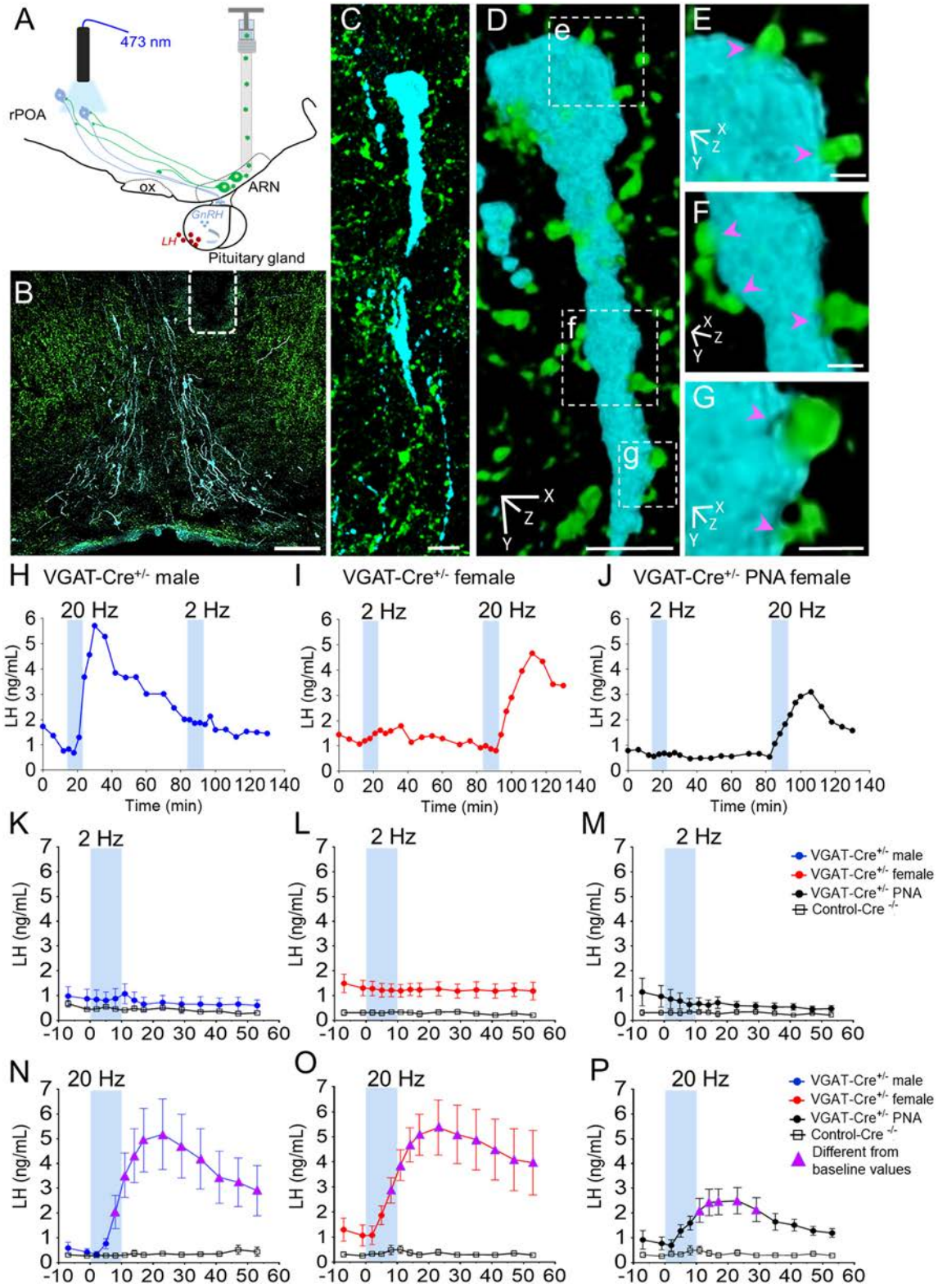

Fig. 2. High frequency optogenetic activation of ARN GABA neuron fibers in the rPOA elicits LH secretion *in vivo*. (*A*) ChETA-assisted circuit mapping is achieved by injecting AAV9-ChETA-eYFP into the ARN of VGAT-Cre mice and subsequently activating ARN GABA neuron fibers projecting into the rPOA, where many GnRH neurons are located. Serial tail-tip blood sampling for LH serves as a proxy for *in vivo* GnRH neuron stimulation. (*B*) Representative confocal images demonstrating optical fiber placement (*white dashed lines*) adjacent to GnRH neurons (*blue*) and AAV9-ChETA-eYFP transfected GABA fibers projecting from the ARN (*green*, scale bar = 100 μm). (*C-G*) Projected confocal image and rotated 3D reconstruction of rPOA GnRH neuron (*blue*) contacted by ChETA-expressing fibers (*magenta arrowheads*, scale bar = 10 μm in C and D, scale bar = 1.5 μm in *E*-G.). (*H-J*) Representative examples of evoked LH secretion following 10 min of 2- and 20-Hz photo-stimulation (*blue bars*) in the rPOA of VGAT-Cre$^{+/-}$ male (*blue symbols*), diestrous female (*red symbols*) and in PNA female mice (*black symbols*) and VGAT-Cre$^{-/-}$ controls (*grey symbols*). (*K—P*) Mean ± SEM LH secretion in VGAT-Cre$^{+/-}$ male (N = 6), diestrous female (*N* = 10), PNA female (*N* = 5) and VGAT-Cre$^{-/-}$ controls (Cre$^{-/-}$ male, N = 5; diestrous female, N = 10; and diestrous PNA, N = 5 mice). Magenta triangles indicate LH levels significantly higher than baseline levels. Two-way ANOVA with Dunnett's *post hoc* test.

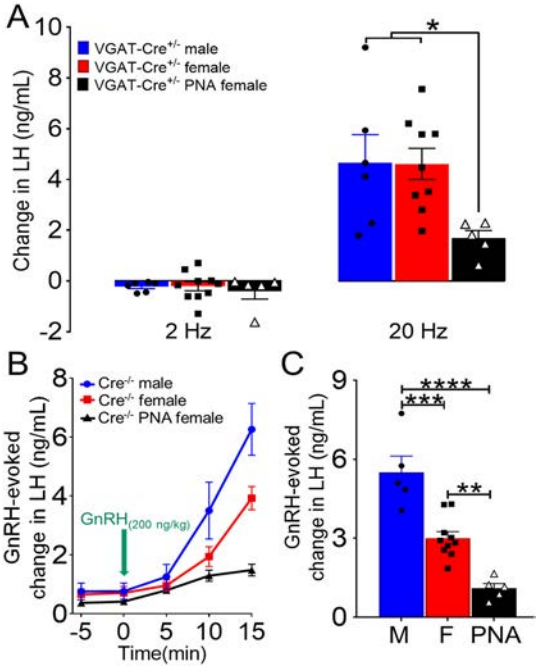

Fig. 3. Optogenetic activation of ARN GABA neuron fibers elicits distinct LH release in normal and PCOS-like mice. (*A*) Histograms show optogenetic-evoked changes in LH levels following 2 Hz and 20 Hz photostimulation of ARN GABA neurons in VGAT-Cre male (N = 6), diestrous female (N = 10) and diestrous PNA (*N* = 5) mice. **p* < .05; one-way ANOVA with Tukey's *post hoc* test was applied for each frequency. (*B*) Dynamics of increased LH release following the injection of s.c. GnRH (200 ng/kg) in $Cre^{-/-}$ mice. (*C*) GnRH-evoked changes in LH release in $Cre^{-/-}$ male (M) (N = 5), diestrous female (F) (N = 10), and diestrous PNA (N = 5) mice. ***p* < .01; ****p* < .001; *****p* < .0001; one-way ANOVA with Tukey's *post hoc* test.

GnRH (200 ng/kg) under isoflurane anesthesia and serial tail tip blood samples were collected to measure LH. Male mice (*N* = 5) showed greater LH release at 10 min (3.5 ± 0.9 ng/mL increase; *p* < .0001) and at 15 min (6.3 ± 0.8 ng/mL increase; *p* < .05) post -GnRH injection compared with diestrous and PNA female mice (Fig. 3*B*). Diestrous female mice (*N* = 10) showed an increase in LH at 15 min, which was significantly greater than PNA female mice (N = 5) (3.9 ± 0.4 *vs.*1.5 ± 0.2 ng/mL increase; *p* < .0001) (Fig. 3*B*). As predicted, analysis of the GnRH-evoked change in LH secretion indicated that PNA female mice exhibit a significantly lower responsiveness of the pituitary gland to exogenous GnRH than male and diestrous female mice ($p < .0001$; $F_{2,17} = 30.14$; one-way ANOVA with Tukey's *post hoc* test) (Fig. 3*C*).

Together, our data support a novel biological role of ARN GABA neurons modulating GnRH/LH secretion *in vivo* in both sexes and in a model of female infertility. These findings indicate that high-frequency photoactivation (20 Hz) of ARN GABA neuron fibers adjacent to GnRH neurons is sufficient to trigger LH release, and that the neuronal firing frequency might be critical to evoke sufficient changes in GnRH neuron activity to promote hormone secretion. Unexpectedly, the activation of ARN GABA neurons promoted a lower magnitude of LH release in PNA female mice that are known to possess increased ARN GABA innervation to the GnRH neurons [26]. However, as PNA animals also exhibited decreased LH secretion in response to exogenous GnRH administration, one explanation of a significantly lower LH response to ARN GABA activation in PNA mice is a smaller LH releasable pool of LH reflecting a history of long-term elevation of LH pulse frequency in the PCOS-like condition [42].

4.3. Optogenetic activation of ARN GABA neuron projections in the rPOA results in variable $GABA_A$-dependent changes in GnRH neuron firing

To directly assess whether ARN GABA projections to the rPOA modulate GnRH neuron firing, acute coronal brain slices were prepared from male, diestrous female, and PNA female VGAT-Cre;GnRH-GFP mice that had received bilateral ARN AAV9-ChETA-eYFP injections. The basal firing rates of rPOA GnRH neurons were not different between male and diestrous female groups (0.137 ± 0.038 Hz in males; 0.135 ± 0.033 Hz in females), but were significantly reduced in PNA mice (0.031 ± 0.017 Hz; *p* < .05 Kruskal Wallis test). The effects on GnRH neuron firing of 2, 10 and 20 Hz blue light activation for 5 min was examined in male and female mice (9–15 cells at each frequency, *N* = 7–8). In all cases, GnRH neurons exhibited four different types of responses; including no response, immediate and transient activation, delayed activation, and immediate inhibition (Table 1, Supplementary Fig. 4). The majority of GnRH neurons exhibited no response (56–70%; Table 1) with an approximately equal distribution of other responses (5–22%) at each frequency in males and females. No significant differences were detected in the response frequency at 2, 10 and 20 Hz or between males and females (*p* > .05; Chi-square test; Table 1). No significant differences were detected in the response frequency at 2, 10 and 20 Hz or between males and females (*p* > .05 Chi-square test; Table 1).

To test the degree to which these responses were dependent upon $GABA_AR$ signalling, an experiment was undertaken in diestrous female mice in which 2, 10 and 20 Hz blue light activation was performed with 5 μM Gabazine, a $GABA_AR$ antagonist, in the aCSF (20 cells from 6 mice). In the presence of GABAzine, no cells exhibited any responses to optogenetic stimulation (Supplementary Fig. 5*A*) indicating that $GABA_A$ receptors are necessary for the variety of responses recorded.

To examine whether changes exist in the impact of ARN GABAergic neurons on rPOA GnRH neurons, a set of optogenetic experiments were undertaken on acute brain slices prepared from PNA female mice. Acute brain slices from normal diestrous female were also examined during the same period. As there was no frequency dependence for GnRH neuron responses to blue light in the *ex vivo* preparation (Table 1), 20 Hz stimulation alone was used for PNA mice. In total, only 2 of 27 GnRH neurons (*N* = 9 PNA mice) responded to blue light and both did so with an immediate activation (Supplementary Fig. 5*B*) The overall percentage of GnRH neurons responding to optogenetic activation of ARN GABAergic fibers in PNA mice (7%) was significantly smaller compared to diestrous female mice ($p < .001$ Chi-$square_{32,3}$; Table 1). The GnRH neurons in PNA mice were found to be able to respond normally to bath applied muscimol, a $GABA_AR$ agonist (*n* = 12 cells), or kisspeptin, a potent stimulator of GnRH neurons (*n* = 3 cells) (Supplementary Fig. 5*B*). These data indicate a $GABA_AR$-dependence for GnRH activity changes in response to activation of ARN GABA fibers in the rPOA and a different responsiveness in PNA animals.

Table 1
Summary of GnRH neuron responses to optogenetic activation. Animal number (N) is given in headings. Numbers of cells responding are given in the table. * p < .001 Chi-$square_{32,3}$ test comparing the proportion of cells showing immediate activation in diestrous females and PNA females.

		2 Hz (N = 7–8)	10 Hz (N = 7–8)	20 Hz (N = 9–12)
Male	No response	6/9 (67%)	5/9 (56%)	14/21 (67%)
	Delayed activation	1/9 (11%)	1/9 (11%)	1/21 (5%)
	Immediate activation	1/9 (11%)	2/9 (22%)	4/21 (19%)
	Immediate inhibition	1/9 (11%)	1/9 (11%)	2/21 (10%)
Female	No response:	7/10 (70%)	9/15 (61%)	18/29 (62%)
	Delayed activation:	1/10 (10%)	2/15 (13%)	5/29 (17%)
	Immediate activation:	1/10 (10%)	2/15 (13%)	4/29 (13%)
	Immediate inhibition:	1/10 (10%)	2/15 (13%)	2/29 (7%)
PNA female	No response:			25/27 (93%)
	Delayed activation:			0/27 (0%)
	Immediate activation:			2/27 (7%)*
	Immediate inhibition:			0/27 (0%)

4.4. Selective targeting and activation of ARN GABA neurons with DREADDs

To assess the impact of chronically elevated ARN GABA neuron activity, VGAT-Cre mice were used to specifically express the DREADDs activator hM3Dq [43] in ARN GABA neurons. AAV5-hM3D(Gq)-mCherry or the control virus AAV5-mCherry were injected bilaterally into the ARN of male and female VGAT-Cre;τGFP reporter mice (Fig. 4*A* and *B*). AAV5-hM3Dq-mCherry transfection was entirely restricted to τGFP-positive cells (Fig. 4*B-G*). Despite very limited injection volumes (100 nL/side), AAV5-hM3Dq-mCherry transfection was frequently not entirely confined to the ARN, with evident expression in various mediobasal hypothalamic nuclei, including the dorsomedial nucleus of the hypothalamus (DMH) and the tuberal nucleus (Supplementary Fig. 6). To overcome this technical challenge and attribute outcomes with the activation of ARN-specific GABA neurons, animals with off target transfection were included as controls. Mice with largely ARN confined transfection and >10 transfected cells/section in the ARN were considered as targeted transfections, referred to as ARN $GABA^{hM3Dq+}$ (Fig. 4, Supplementary Table 2). Mice with fewer than 10 transfected cells throughout the ARN and transfection in areas outside of the ARN were considered off target controls, referred to as ARN $GABA^{OFF\ Target}$. The average number of hM3Dq-mCherry immunoreactive cells per section throughout the rostral to caudal extent of the ARN was 39.62 ± 6.6 in ARN $GABA^{hM3Dq+}$ mice and 3.01 ± 1.4 in ARN $GABA^{OFF\ Target}$ mice (Supplementary Table 2).

To validate the efficacy of the DREADDs activator hM3Dq to activate ARN GABA neurons with designer drug, clozapine N-oxide (CNO), administration, acute coronal brain slices (250-μm thick) encompassing the ARN were prepared for cell-attached recordings from VGAT-Cre;τGFP neurons in male mice ($N = 3$) that had been previously bilaterally transfected with AAV5-hM3Dq-mCherry in the ARN. Delivery of 1 μM CNO into the bath elicited a significant increase in firing rate in all ARN GABA neurons expressing hM3Dq-mCherry ($n = 6$ cells, $p = .03$, Fig. 4*H* and *I*).

4.5. Local chemogenetic activation of ARN GABA neurons in vivo stimulates LH secretion

We first examined whether the effect of acute, local hM3Dq-mediated activation of ARN GABA terminals in the rPOA was similar to that observed with optogenetic stimulation. Male and female VGAT-Cre;τGFP mice with bilateral transfection of AAV5-hM3Dq-mCherry in the ARN were anesthetized and a cannula was targeted to the rPOA to deliver CNO or aCSF (Fig. 5*A*). As with ChETA transfection, hM3Dq transfected ARN GABA fibers were found throughout the rPOA and in close apposition with GnRH neuron cell bodies and dendrites (Fig. 5*B* and *C*). CNO (30 μM) or aCSF was delivered into the rPOA of anesthetized male and female mice and serial tail-tip blood samples were collected to measure LH release, as a proxy of GnRH release (Fig. 5*D*). Post-mortem immunohistochemical analysis classified experimental groups as those with clear ARN-located transfection and an rPOA located needle track (ARN $GABA^{hM3Dq+}$/$rPOA^{ON}$) and controls as those with off target transfection (ARN $GABA^{OFF\ Target}$/$rPOA^{ON}$) or off target rPOA needle placement (ARN $GABA^{hM3Dq+}$/$rPOA^{OFF}$).

Delivery of CNO had little impact on LH secretion in controls, which included ARN $GABA^{OFF\ Target}$/$rPOA^{ON}$ ($N = 4$ males and $N = 12$ females, Supplementary Fig. 7*A* and *B*), or mice transfected with control virus (ARN $GABA^{AAV\text{-}mCherry}$, N = 4 males and $N = 3$ females, Supplementary Fig. 7 *A* and *B*). Delivery of aCSF to ARN $GABA^{hM3Dq+}$/$rPOA^{ON}$ mice (N = 4 males and $N = 2$ females, Supplementary Fig. 7 *A* and *B*) also did not change LH secretion. In contrast, CNO delivery to the rPOA in ARN $GABA^{hM3Dq+}$/$rPOA^{ON}$ mice elicited a significant increase in LH secretion in both males ($N = 6$, Fig. 5*G* and *I*) and diestrus females ($N = 5$, Fig. 5*H* and *J*) compared with controls (Fig. 5*E* and *F*). Statistical analysis of the mean circulating LH level compared to the baseline before CNO injection showed that circulating LH levels were significantly increased in males ($p < .0001$, $F_{15,\ 240} = 3.376$) and diestrous females ($p < .0001$, $F_{15,\ 300} = 8.697$) (Fig. 5*I* and *J*). Multiple

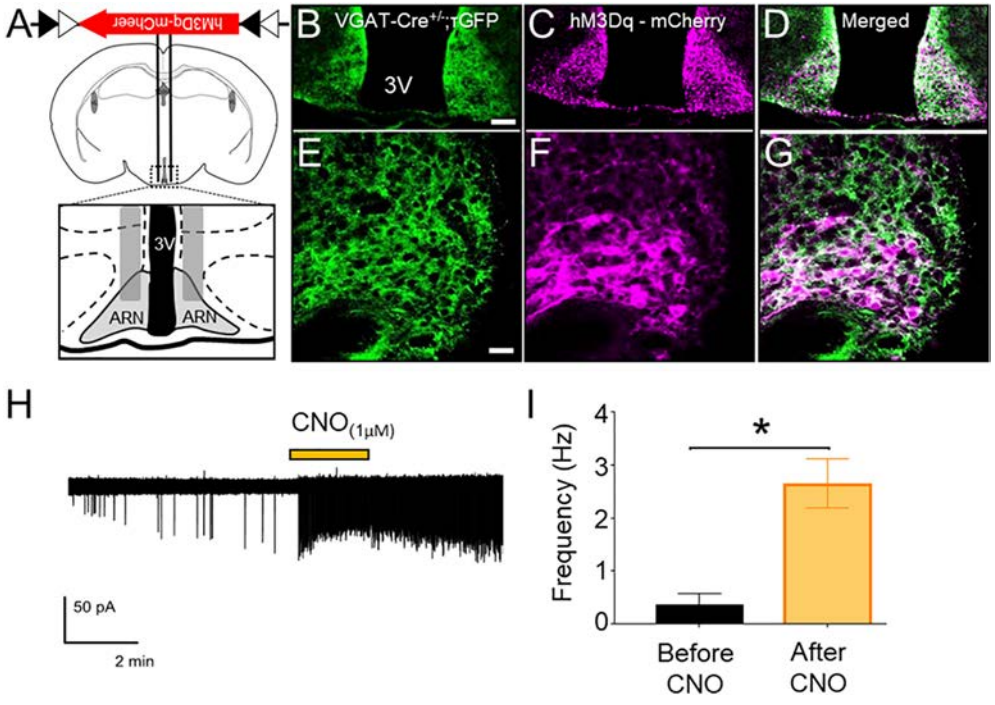

Fig. 4. Selective targeting and activation of ARN GABA neurons with the chemogenetic activator hM3Dq. (*A,B*) Schematic of the coronal mouse brain depicting the ARN location of bilateral AAV5-hM3Dq-mCherry injection. (*C-G*) Representative confocal images showing τGFP reporter expression of VGAT cells (*green*), AAV5-hM3Dq-mCherry transfected cells (*magenta*) and co-localization (*white*) in the ARN at low and high magnification (scale bar in *B-D* = 100 μm, in *E-G* = 25 μm). (*H*) Cell-attached recordings from hM3Dq-mCherry-expressing neurons in the ARN. Yellow bar indicates the time of 1 μM CNO administration to the bath. (*I*) Mean ± SEM firing frequencies before and after CNO administration to hM3Dq-mCherry-expressing neurons in brain slices from VGAT-Cre;τGFP male mice ($n = 6$ cells from 3 animals). $^*p < .05$; Wilcoxon matched pairs signed rank test.

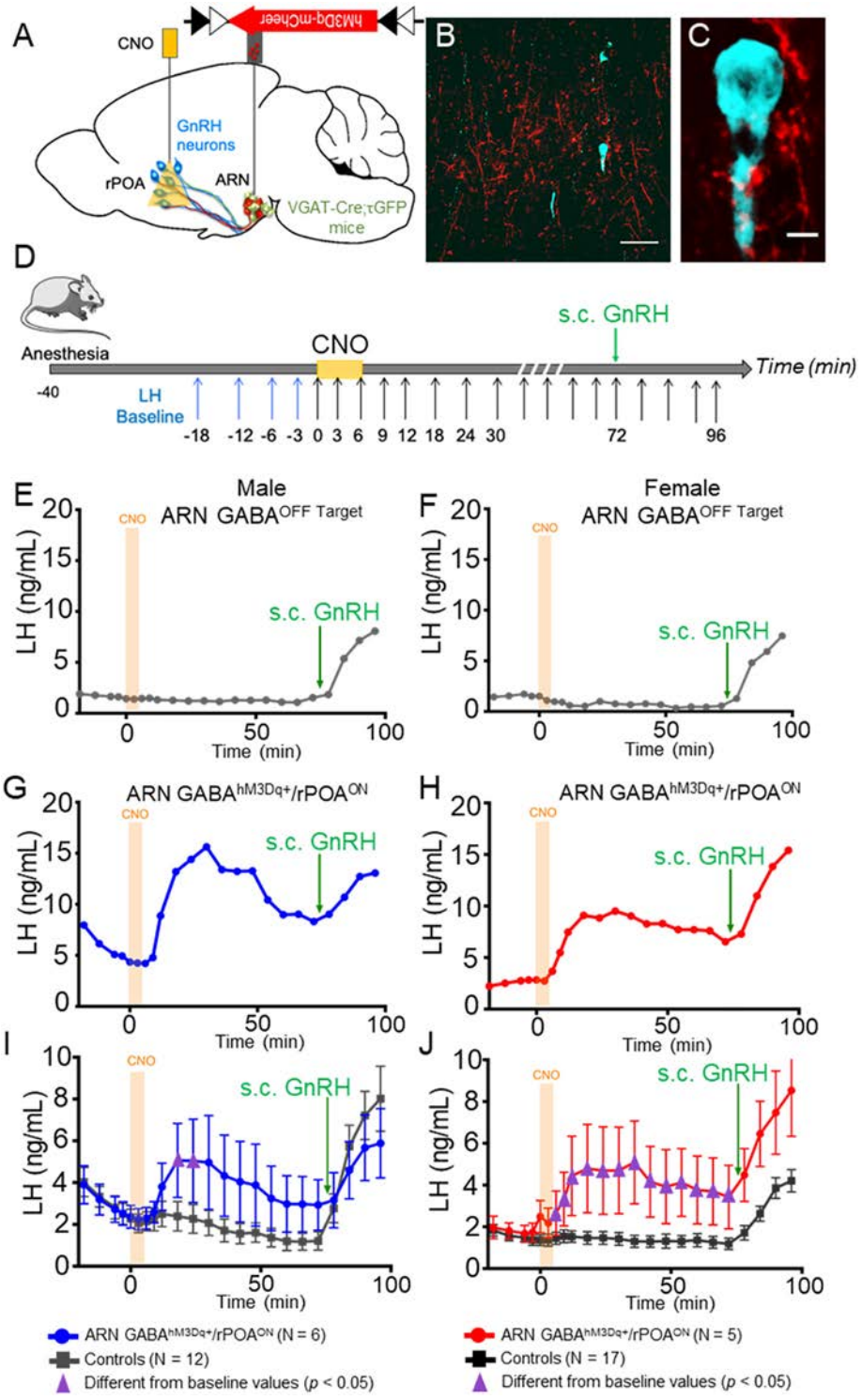

Fig. 5. CNO administration to hM3Dq-expressing ARN GABA neuron fibers in the rPOA elicits LH secretion in male and female mice. (*A*) Schematic of the regions targeted in a sagittal mouse brain map for transfection and CNO delivery. (*B,C*) Representative confocal images showing ARN GABA projecting fibers transfected with AAV5-hM3Dq-mCherry (*red*) nearby GnRH neurons (*blue*) in the rPOA at low and high magnification. Scale bar in $B = 100$ μm and in $C = 5$ μm. (*D*) Protocol timeline. (*E,F*) Representative LH secretion pattern from ARN $GABA^{OFF\ Target}$ male and female controls in response to CNO delivery and peripheral GnRH administration. (*G,H*) Representative examples of circulating LH secretion patterns in response to CNO delivery into the rPOA of correctly targeted ARN $GABA^{hM3Dq+}/rPOA^{ON}$ male (blue traces) and female (red traces) mice. (*I-J*) Mean ± SEM LH responses in ARN $GABA^{hM3Dq+}/rPOA^{ON}$ males (blue) and females (red) and in corresponding control animals (grey). Purple triangles indicate LH levels significantly higher ($p < .05$) than baseline levels. Two-way ANOVA with Dunnett's *post hoc* test.

comparisons post-hoc test showed that mean LH levels are significantly increased from baseline at 12 and 18 min after CNO injection in ARN $GABA^{hM3Dq+}/rPOA^{ON}$ males (Fig. 5*I*, respectively $p = .04$ and $p = .04$) and from 6 to 72 min after CNO injection in ARN $GABA^{hM3Dq+}/rPOA^{ON}$ females (Fig. 5*J*; at 6 min, $p = .005$; at 12–60 min, $p = .0001$; at 6–72 min, $p = .002$).

4.6. Chronic activation of ARN GABA neurons partially recapitulates a PCOS-like condition

Given the *in vitro* and *in vivo* data indicating that chemogenetic tools were capable of activating ARN GABA neurons, we then tested the impact of chronic ARN GABA neuron activation on downstream reproductive function. We hypothesized that chronic activation of ARN GABA neurons in healthy female mice would disrupt fertility and increase LH and testosterone secretion similar to the PCOS-like condition. Three weeks after VGAT-Cre;τGFP female mice were bilaterally transfected with AAV-hM3Dq-mCherry or the control vector AAV-mCherry, they were placed in cages where they received *ad libitum* drinking water only for 2–3 weeks followed by drinking water with CNO (5 mg/kg/day) for 2–3 weeks (Fig. 6*A*). Variation in treatment time was due to variation in estrous cycle stage timing for LH pulse frequency data collection. As before, controls consisted of VGAT-Cre;τGFP ARN GABA$^{\text{OFF Target}}$ (N =

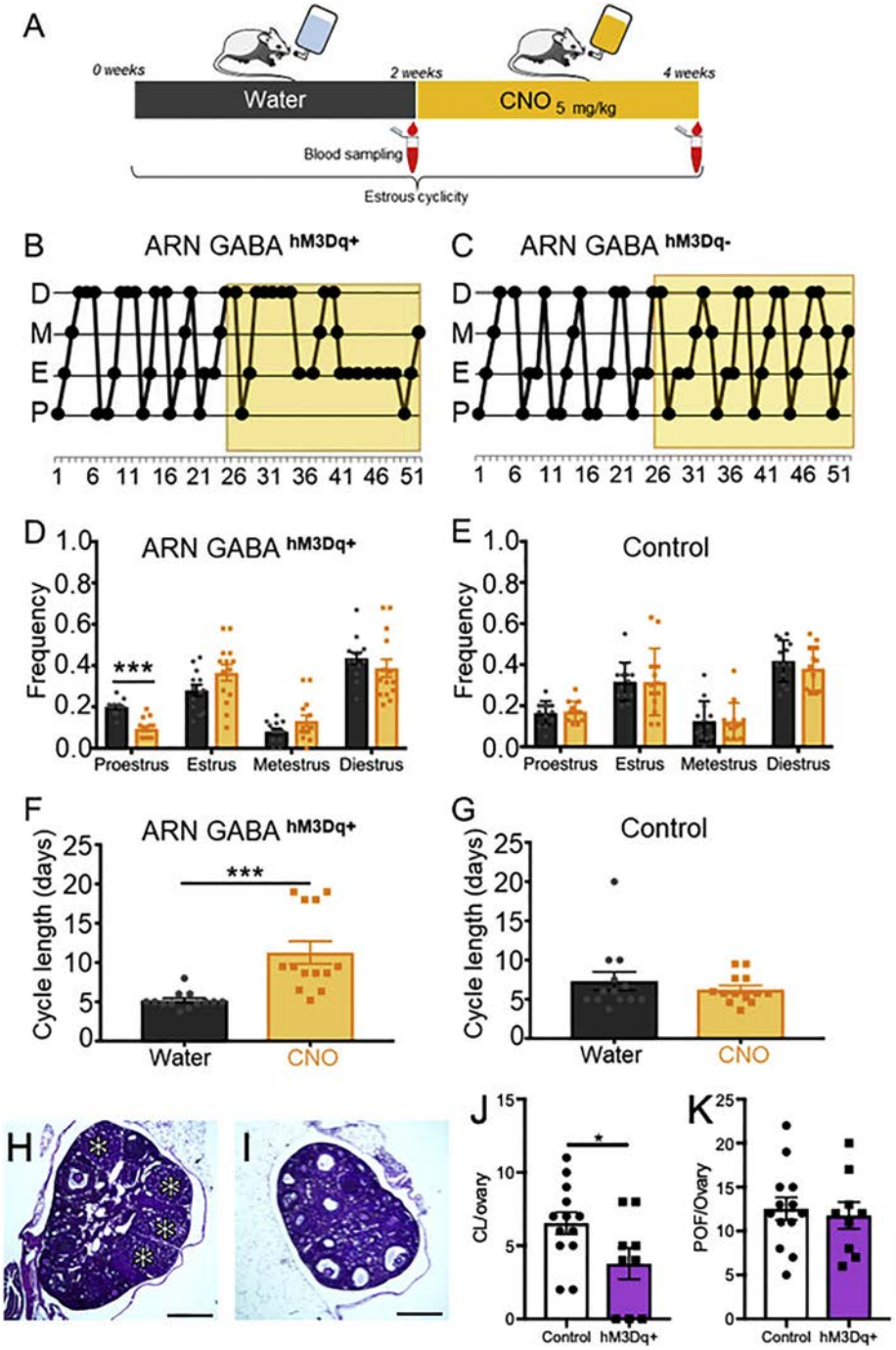

Fig. 6. Chronic exposure to CNO activation of ARN GABA neurons disrupts estrus cyclicity in female mice. (*A*) Schematic of the protocol to chronically activate hM3Dq-expressing ARN GABA neurons with CNO administration through the drinking water. (*B,C*) Representative examples of estrous cyclicity before and during CNO (yellow box) exposure in an ARN GABA$^{\text{hM3Dq+}}$ female and in a ARN GABA$^{\text{OFF Target}}$ control animal. (*D,E*) Mean ± SEM frequency of each estrous cycle phase before (water; grey bars) and during CNO exposure (CNO; yellow bars) in ARN GABA$^{\text{hM3Dq+}}$ females ($N = 13$) and in control animals (N = 13, consisting of ARN GABA$^{\text{OFF Target}}$ and ARN GABA$^{\text{mCherry}}$ female mice). (*F,G*) Mean ± SEM cycle length in days before and during CNO exposure. (*H—K*) Representative images of ARN GABA$^{\text{mCherry}}$ (*H*) and ARN GABA$^{\text{hM3Dq+}}$ (*I*) ovarian histology; corpora lutea marked with asterisks (*). Mean ± SEM number of preovulatory follicles (POF; *J*) and corpora lutea (CL; *K*) from control (ARN GABA$^{\text{mCherry}}$ and ARN GABA$^{\text{OFFTarget}}$; N = 13) and ARN GABA$^{\text{hM3Dq+}}$ ($N = 9$) mice following CNO administration. * $p < .05$; *** $p < .001$; (*D,E*) Multiple Student's *t*-tests; (*F,G*) Mann-Whitney *U* test; (*J,K*) Student's *t*-tests.

5 females) and ARN GABA$^{AAV\text{-}mCherry}$ ($N = 8$ females). Vaginal cytology was collected daily to assess estrous cycle stage. A typical 4–5-day cycle was observed in all animals with drinking water only. The addition of CNO in the drinking water resulted in significantly disrupted cycles in ARN GABA^{hM3Dq+} mice (Fig. 6*B*) compared with control animals that continued to cycle normally (Fig. 6*C*). Specifically, the frequency of the proestrous stage of the cycle, as indicative of ovulation, was significantly decreased in ARN GABA^{hM3Dq+} mice under CNO treatment compared to water only (Fig. 6*D*; $N = 13$, $p < .001$, df = 25). Specifically, ARN GABA-$^{hM3Dq+}$ mice exhibited extended periods of diestrous or estrous smears, similar to what has been reported previously for PNA mice [20,21,25]. CNO had no effect on cycle stage frequency in control animals (N = 13; Fig. 6*E* and Supplementary Fig. 8; $p = .97$, df = 24). Similarly, the overall estrous cycle length was increased by CNO compared to water only in ARN GABA^{hM3Dq+} mice (Fig. 6*F*; N = 13; $p < .001$, U = 5), while CNO had no effect on cycle length in control animals (Fig. 6*G* and Supplementary Fig. 8). Post-mortem assessment of ovarian histology demonstrated that chronic activation of ARN GABA neurons resulted in a significantly decreased number of corpora lutea (Fig. 6*H-J*). The number of preovulatory follicles was not different (Fig. 6*H,I,K*), and follicle wall cell layer thickness was not statistically significantly different (Supplementary Fig. 9, for granulosa cell layer thickness $p = .059$, 95% confidence interval −9.3 to 0.2).

Serial tail tip blood sampling was performed at the end of the water and CNO treatment periods to assess circulating testosterone and pulsatile LH secretion. In control and ARN GABA^{hM3Dq+} mice, CNO administration had no significant impact on mean circulating testosterone levels (Fig. 7*A* and *B*). However, the percentage change in testosterone in response to CNO was significantly greater in ARN GABA^{hM3Dq+} mice than in controls (Fig. 7*C*; $p < .001$), linking long-term ARN GABA activation with an increase in testosterone production. In addition, we investigated whether chronic activation of ARN GABA neurons were able increase LH secretion. Cumulative LH secretion (area under the curve) from serial blood samples (every 6 min over 2 h) was not different between groups, and chronic activation of transfected ARN GABA neurons with CNO resulted in a non-significant increase in mean LH pulse frequency ($p = .051$, 95% confidence interval −0.0056 to 1.096, Fig. 7*I* and *J*). On balance, these findings support the hypothesis that increased activity in ARN GABA neurons can impair reproductive function in a manner resembling a PCOS-like state.

5. Discussion

Our results demonstrate that selective stimulation of ARN GABA neurons can activate the hypothalamic-pituitary axis. We provide evidence, using both optogenetic and chemogenetic tools, that selective activation of ARN GABA fibers surrounding GnRH neurons elicits robust LH secretion in both males and females. A similar stimulation of LH secretion was observed in prenatally androgenised PCOS-like mice, previously shown to exhibit elevated input from ARN GABA neurons [19–21,26], although the magnitude of release was surprisingly lower than that of healthy males and females. At a cellular level, GnRH neuron responses to ARN GABA fiber activation were infrequent and variable, but all responses were $GABA_A$ dependent. At the systems level, long-term activation of the ARN GABA circuit was found to disrupt reproductive cycles, reduce the number of corpora lutea and stimulate increased

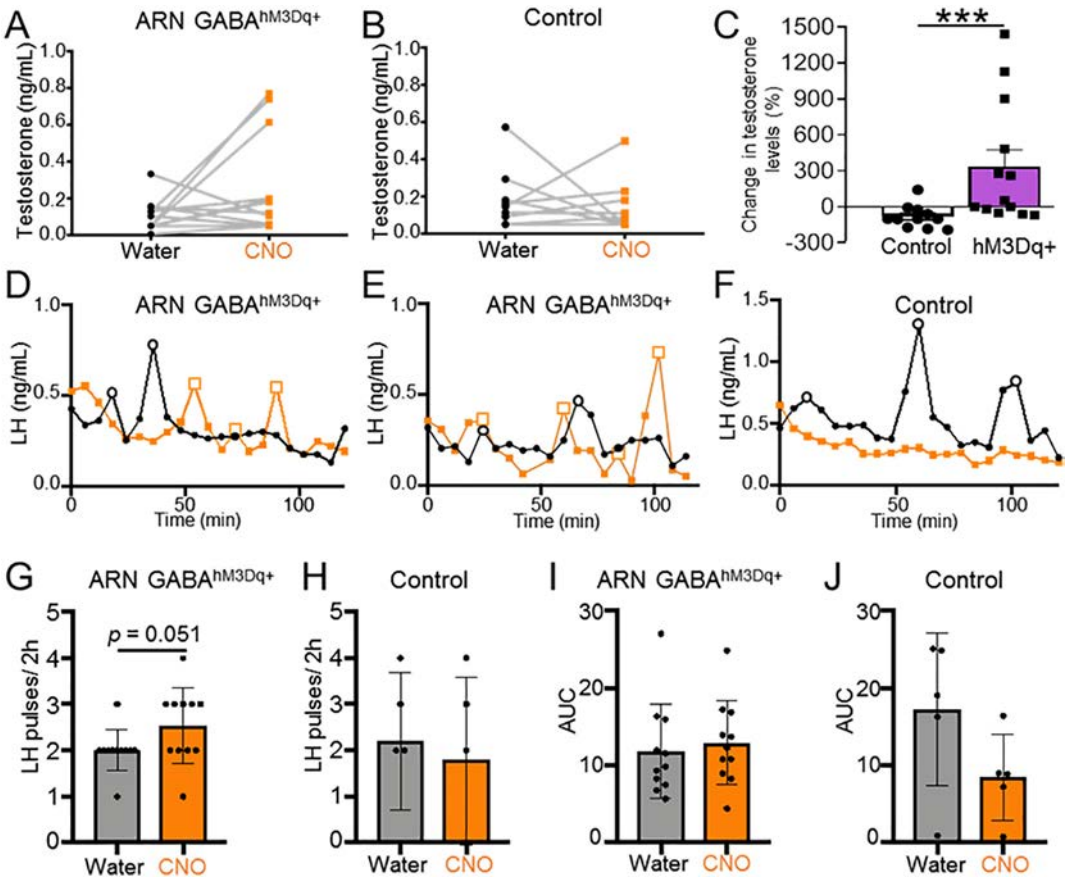

Fig. 7. The effect of chronic ARN GABA neuron activation on testosterone and LH pulse frequency in female mice. (*A,B*) Individual levels of circulating testosterone levels before (black dots) and during treatment with CNO in the drinking water (orange squares) in ARN GABA $^{hM3Dq+}$ (N = 13) and controls (consisting of ARN GABA$^{OFF\ Target}$ ($N = 5$) and ARN GABA^{mCherry} ($N = 6$) mice. (*C*) Percentage change in testosterone in response to CNO compared between control and ARN GABA^{hM3Dq+} mice. (*D-F*) Representative examples of LH release profiles over 2 h in individual ARN GABA $^{hM3Dq+}$ and ARN GABA$^{OFF\ Target}$ animals at the end of 2 weeks of water only (black line and dots) and then following 2 weeks of CNO administration through the drinking water (orange line and square). (*G,H*) LH pulse frequency before and after CNO treatment period, and (*I,J*) cumulative LH secretion (area under the curve) before and after CNO treatment period in ARN GABA $^{hM3Dq+}$ ($N = 11$) and ARN GABA$^{OFF\ Target}$ (N = 5) groups. (*A,B,G-J*) Paired Student's *t*-tests; (C) Mann-Whitney *U* test; *** $p < .001$.

testosterone production otherwise healthy females. These findings support the hypothesis that ARN GABA neurons are a functional component of the GnRH neuronal network in both males and females and suggest that elevated activity in this circuit can drive dysfunction in the central regulation of fertility. However, the smaller magnitude GnRH/LH response in PNA mice mimicking PCOS suggests that the ARN GABA-to-GnRH circuit behaves differently in the PCOS-like state and that the neuroendocrine dysfunction of PCOS likely involves additional circuit abnormalities. These preclinical data are relevant to the human condition as they aid in discerning the underappreciated and critical function of the brain in the pathogenesis of PCOS.

We confirmed that the ChETA channelrhodopsin variant, used previously to activate fast spiking GABA neurons [44,45], also exhibits high spike fidelity in ARN GABA neurons. The AAV9 vector enabled restricted, robust and specific expression of ChETA within VGAT-positive neurons of the ARN and their projections. Stimulation of LH secretion *in vivo* occurred only in response to high frequency light stimulation (20 Hz), which evoked a slow-onset, high magnitude, long lasting elevation in LH secretion *in vivo* that was not different between males and females. *In vitro*, approximately 30% of GnRH neurons responded to ARN GABA fiber photostimulation, and responses were observed at all frequencies tested (2, 10 and 20 Hz). Previously, optogenetic activation of pre-optic GABA neurons has been shown to stimulate both delayed and immediate responses in approximately 50% of GnRH neurons at 2 and 10 Hz [46]. The low response rate of GnRH neurons here to ARN GABA fiber stimulation may reflect technical limitations, including the inability to determine whether patched cells are indeed postsynaptic to ChETA-expressing ARN GABA fibers. However, the lack of frequency dependence to ARN GABA fiber stimulation for a variety of response types suggests that the downstream responses to ARN GABA stimulation are also complex. ARN GABA neurons are heterogeneous and synthesize a vast array of neurotransmitters [38,47,48], making it difficult to predict the specific neurotransmitters that are secreted following high frequency optogenetic stimulation. Optogenetic activation of rPOA-located GABA neurons evokes an immediate GnRH neuron excitation at low frequencies, attributed to GABA, and a delayed, long-lasting activation at higher frequency stimulation, attributed to kisspeptin release [46]. While high frequency optogenetic stimulation is associated with neuropeptide secretion and low frequency activation results in classic small molecule neurotransmission [46,49], high frequency stimulation is also associated with postsynaptic responses that are dependent upon $GABA_AR$ signalling [50]. While it will be important, as tools develop, to assess the full repertoire of neurotransmitter secretion responsible for the GnRH and LH responses observed here, the complete lack of GnRH responses in the presence of the $GABA_AR$ blocker GABAzine in *ex vivo* preparations suggest that GABA is likely a critical component in the functional ARN GABA to GnRH neuron circuit.

The smaller magnitude and duration of LH secretion in PCOS-like mice following activation of ARN GABA terminals was unexpected, particularly given the increased GABA activity and GABA innervation specifically from the ARN to GnRH neurons evident in this model [26]. However, LH release in response to exogenous GnRH administration was also significantly diminished in these mice. GnRH stimulated significantly different levels of LH release in male, female and PNA mice that is inversely associated with their typical LH pulse frequency [33,35]. In other species, diminished LH synthesis and secretion is associated with periods of high frequency GnRH stimulation, including in the non-human primate [51] and the ewe [42]. The prenatally androgenised mouse model of PCOS is reported to exhibit both increased LH pulse frequency [26] and increased GnRH neuron firing frequency [19,52]. Therefore, the reduced LH response to both ARN GABA stimulation and GnRH in PNA mice may reflect a history of hyperactive GnRH neuron activity and secretion. It is also important to note that optogenetic activation of ARN GABA neurons promoted robust LH release, reaching levels greater than plasma LH levels typically found in PNA mice [26]. Therefore, this artificially-induced LH release may lead to a rapid discharge of readily available LH vesicles in the pituitary gland, which are already diminished in the PCOS-like condition of historically high GnRH stimulus. The reduced basal firing rate and response to GABAergic optogenetic activation of GnRH neurons in PNA mice found here was surprising given indications for increased GnRH neuron firing shown previously in the same model [19,52]. An alternative hypothesis to explain reduced GnRH and LH responses to ARN GABA fiber stimulation in PNA animals may be the indirect involvement of as yet undefined local circuits that are also wired differently in the PNA animal.

Increased LH secretion was also evident following local chemogenetic activation of ARN GABA fibers in the rPOA of male and female mice. The response in males was more variable than in females, with females exhibiting consistently elevated LH release for over an hour. No sex differences were observed following optogenetic stimulation and there is no evidence for sex differences in GABAergic input to GnRH neurons [36]. Despite using the same Cre driver line, the spread and density of transfection with the AAV5-hSyn-DiO-hM3D(Gq)-mCherry vector was very different to the transfection observed with the ChETA vector. Despite very small volumes injected, the spread of hM3Dq transfection was difficult to entirely restrict to the ARN, which may be due to differences in tissue-specific tropism between AAV5 and AAV9 [53]. Also, while ChETA transfection was robust, targeting in excess of 200 VGAT-positive neurons per slice throughout out the ARN, hM3Dq transfection only targeted roughly 40 cells per section. However, even this limited number of transfected cells resulted in a network of hM3Dq-expressing projections to GnRH neurons in the rPOA. Lack of an LH response to CNO in animals with hM3Dq-expressing GABA neurons outside of the ARN suggests that stimulation of the GnRH/LH axis is specific to GABAergic neurons located in the ARN.

Although selective activation of the ARN to rPOA GABA circuit resulted in blunted GnRH and LH responses, we subsequently found that chronic elevation in ARN GABA neuron activity resulted in reproductive dysfunction similar to a PCOS-like state [20,21,25]. Two weeks of chronic activation, induced *via* CNO intake in the water, led to impaired estrous cycles, evident in decreased or absent proestrous days and a significant reduction in corpora lutea structures in the ovary. Importantly, disrupted estrous cyclicity was not due to inhibition of the HPG axis as animals continued to exhibit LH pulses after 2 weeks of chronic ARN GABA activation. In fact, a non-significant increase in mean LH pulse frequency ($p = .051$) was observed, suggestive of elevations in LH similar to those identified in women with PCOS [6,10] and in the PNA PCOS-like model [26]. This was accompanied by a proportional increase in testosterone levels that was significantly greater to that seen in controls. A significant decrease in corpora lutea number is suggestive of impairments in ovulation. These data support the link between elevated activity in the ARN GABA circuit and the development of PCOS-like impairments in the neuroendocrine regulation of fertility. These findings provide a potential mechanism explaining the development of PCOS features in women following treatment with GABA-acting anti-epileptic drugs [54].

Several questions remain to be determined, including how activation of ARN GABA neurons impacts FSH levels. Increased GnRH pulse frequency favours pituitary synthesis of LH over FSH, and an increased LH to FSH ratio is commonly seen in women with PCOS [5]. Anovulation in women with PCOS results from insufficient levels of FSH to support folliculogenesis, and exogenous treatments that increase FSH for the appropriate duration can restore folliculogenesis and ovulation in women with PCOS [55–57]. It will be important in future studies to identify the impact of prenatal androgen excess and associated alterations in the GnRH neuronal network on FSH secretion. In addition, given the growing evidence demonstrating clinical implications for sons of PCOS mothers [58], it will be important to understand how prenatal androgen excess impacts the GnRH neuronal network and HPG axis function of male offspring. Prenatally androgenized male mice exhibit increased spontaneous GABAergic neurotransmission to GnRH neurons at four

weeks of age [19]. It will be of interest to determine whether this is associated with GABAergic wiring changes as in females [26] and whether chronic elevations in ARN GABA activity impact reproductive function. Finally, as clinical PCOS is frequently associated with both hyperandrogenism and hyperinsulinemia, it will be important to determine the individual and combined impact of these features on GABAergic function.

In summary, we provide here a collective body of cellular and systems evidence supporting the functional importance of ARN GABA neurons in reproductive health and dysfunction. The stimulatory effect of ARN GABA activation on the HPG axis and the reproductive impairments that arise following a chronic increase in ARN GABA tone support the hypothesis that GABA innervation to GnRH neurons originating from the ARN could underpin the hyperactive GnRH/LH axis in the PCOS-like condition. These data hint at brain mechanisms that could become future therapeutic targets for the diagnosis and/or treatment of PCOS. The unexpectedly blunted HPG axis responses in PCOS-like mice with reported enhancement of GABA innervation to GnRH neurons raises questions about impaired function within the ARN GABA population, as well as questions about the involvement of other circuits. Additionally, the temporal requirements for the development of the PCOS phenotype following enhanced ARN GABA signalling will be important to address in the future. As the critical components of the GnRH neuronal network that are altered in PCOS are mechanistically defined, opportunities will arise to better understand the etiology of PCOS and how to best treat this common female disorder going forward.

Acknowledgements

We thank Dr. Bradford Lowell (Harvard Medical School) for the kind provision of transgenic mice, Leo van Rens of EMTech (University of Otago) for technical assistance, Otago Histology Services for technical assistance, and Dr. Su Y. Han and Dr. Pauline Campos for their technical assistance with technical development.

Funding sources

This study was funded by the Marsden Fund of the Royal Society, the Health Research Council of New Zealand, and the University of Otago. Funders had no role in study design; in the collection, analysis, and interpretation of data; in the writing of the report; and in the decision to submit the paper for publication.

Declaration of interests

The authors have no conflicts of interest to disclose.

Author contributions

Mauro Silva: Data curation; Formal analysis; Validation; Investigation; Methodology; Writing (original draft; review and editing).

Elodie Desroziers: Data curation; Formal analysis; Validation; Investigation; Methodology; Writing (original draft; review and editing).

Sabine Hessler: Data curation; Formal analysis; Investigation; Methodology; Writing (original draft).

Melanie Prescott: Data curation; Formal analysis; Investigation; Methodology; Project administration.

Chris Coyle: Data curation; Formal analysis; Investigation; Methodology.

Allan Herbison: Conceptualization; Resources; Supervision; Methodology; Writing—original draft; Project administration.

Rebecca Campbell: Conceptualization; Resources; Data curation; Supervision; Funding acquisition; Methodology; Project administration; Writing (original draft; review and editing).

Appendix A. Supplementary data

Supplementary data to this article can be found online at https://doi.org/10.1016/j.ebiom.2019.05.065.

References

[1] Stamatiades GA, Kaiser UB. Gonadotropin regulation by pulsatile GnRH: signaling and gene expression. Mol Cell Endocrinol 2018;463:131–41.
[2] Herbison AE. The gonadotropin-releasing hormone pulse generator. Endocrinology 2018;159(11):3723–36.
[3] Campbell RE. Defining the gonadotrophin-releasing hormone neuronal network: transgenic approaches to understanding neurocircuitry. J Neuroendocrinol 2007;19(7):561–73.
[4] Herbison AE. Physiology of the adult gonadotropin-releasing hormone neuronal network. In: Zeleznik PlantTM, J A, editors. Knobil and Neil's physiology of reproduction. 4th ed. New York: Elsevier Academic Press; 2015. p. 399–468.
[5] Taylor AE, McCourt B, Martin KA, et al. Determinants of abnormal gonadotropin secretion in clinically defined women with polycystic ovary syndrome. J Clin Endocrinol Metab 1997;82(7):2248–56.
[6] Berga SL, Guzick DS, Winters SJ. Increased luteinizing hormone and alpha-subunit secretion in women with hyperandrogenic anovulation. J Clin Endocrinol Metab 1993;77(4):895–901.
[7] Pastor CL, Griffin-Korf ML, Aloi JA, Evans WS, Marshall JC. Polycystic ovary syndrome: evidence for reduced sensitivity of the gonadotropin-releasing hormone pulse generator to inhibition by estradiol and progesterone. J Clin Endocrinol Metab 1998;83(2):582–90.
[8] Daniels TL, Berga SL. Resistance of gonadotropin releasing hormone drive to sex steroid-induced suppression in hyperandrogenic anovulation. J Clin Endocrinol Metab 1997;82(12):4179–83.
[9] Eagleson CA, Gingrich MB, Pastor CL, et al. Polycystic ovarian syndrome: evidence that flutamide restores sensitivity of the gonadotropin-releasing hormone pulse generator to inhibition by estradiol and progesterone. J Clin Endocrinol Metab 2000;85(11):4047–52.
[10] Yoo RY, Dewan A, Basu R, Newfield R, Gottschalk M, Chang RJ. Increased luteinizing hormone pulse frequency in obese oligomenorrheic girls with no evidence of hyperandrogenism. Fertil Steril 2006;85(4):1049–56.
[11] Patel K, Coffler MS, Dahan MH, et al. Increased luteinizing hormone secretion in women with polycystic ovary syndrome is unaltered by prolonged insulin infusion. J Clin Endocrinol Metab 2003;88(11):5456–61.
[12] Nelson VL, Qin KN, Rosenfield RL, et al. The biochemical basis for increased testosterone production in theca cells propagated from patients with polycystic ovary syndrome. J Clin Endocrinol Metab 2001;86(12):5925–33.
[13] Rosenfield RL, Ehrmann DA. The pathogenesis of polycystic ovary syndrome (PCOS): the hypothesis of PCOS as functional ovarian Hyperandrogenism revisited. Endocr Rev 2016;37(5):467–520.
[14] Burt Solorzano CM, Beller JP, Abshire MY, Collins JS, McCartney CR, Marshall JC. Neuroendocrine dysfunction in polycystic ovary syndrome. Steroids 2012;77(4):332–7.
[15] Moore AM, Campbell RE. Polycystic ovary syndrome: understanding the role of the brain. Front Neuroendocrinol 2017;46:1–14.
[16] Roland AV, Moenter SM. Reproductive neuroendocrine dysfunction in polycystic ovary syndrome: insight from animal models. Front Neuroendocrinol 2014;35(4):494–511.
[17] Berga SL, Yen SS. Opioidergic regulation of LH pulsatility in women with polycystic ovary syndrome. Clin Endocrinol 1989;30(2):177–84.
[18] Kawwass JF, Sanders KM, Loucks TL, Rohan LC, Berga SL. Increased cerebrospinal fluid levels of GABA, testosterone and estradiol in women with polycystic ovary syndrome. Hum Reprod 2017;32(7):1450–6.
[19] Berg T, Silveira MA, Moenter SM. Prepubertal development of GABAergic transmission to gonadotropin-releasing hormone (GnRH) neurons and postsynaptic response are altered by prenatal Androgenization. J Neurosci 2018;38(9):2283–93.
[20] Sullivan SD, Moenter SM. Prenatal androgens alter GABAergic drive to gonadotropin-releasing hormone neurons: implications for a common fertility disorder. Proc Natl Acad Sci U S A 2004;101(18):7129–34.
[21] Silva MS, Prescott M, Campbell RE. Ontogeny and reversal of brain circuit abnormalities in a preclinical model of PCOS. JCI Insight 2018;3(7).
[22] DeFazio RA, Heger S, Ojeda SR, Moenter SM. Activation of A-type gamma-aminobutyric acid receptors excites gonadotropin-releasing hormone neurons. Mol Endocrinol 2002;16(12):2872–91.
[23] Herbison AE, Moenter SM. Depolarising and hyperpolarising actions of GABA (a) receptor activation on gonadotrophin-releasing hormone neurones: towards an emerging consensus. J Neuroendocrinol 2011;23(7):557–69.
[24] Vong L, Ye C, Yang Z, Choi B, Chua Jr S, Lowell BB. Leptin action on GABAergic neurons prevents obesity and reduces inhibitory tone to POMC neurons. Neuron 2011;71(1):142–54.
[25] Moore AM, Prescott M, Campbell RE. Estradiol negative and positive feedback in a prenatal androgen-induced mouse model of polycystic ovarian syndrome. Endocrinology 2013;154(2):796–806.
[26] Moore AM, Prescott M, Marshall CJ, Yip SH, Campbell RE. Enhancement of a robust arcuate GABAergic input to gonadotropin-releasing hormone neurons in a model of polycystic ovarian syndrome. Proc Natl Acad Sci U S A 2015;112(2):596–601.
[27] Moore AM, Campbell RE. The neuroendocrine genesis of polycystic ovary syndrome: a role for arcuate nucleus GABA neurons. J Steroid Biochem Mol Biol 2016;160:106–17.

[28] Gunaydin LA, Yizhar O, Berndt A, Sohal VS, Deisseroth K, Hegemann P. Ultrafast optogenetic control. Nat Neurosci 2010;13(3):387–92.
[29] Madisen L, Zwingman TA, Sunkin SM, et al. A robust and high-throughput Cre reporting and characterization system for the whole mouse brain. Nat Neurosci 2010;13(1):133–40.
[30] Wen S, Gotze IN, Mai O, Schauer C, Leinders-Zufall T, Boehm U. Genetic identification of GnRH receptor neurons: a new model for studying neural circuits underlying reproductive physiology in the mouse brain. Endocrinology 2011;152(4):1515–26.
[31] Spergel DJ, Kruth U, Hanley DF, Sprengel R, Seeburg PH. GABA- and glutamate-activated channels in green fluorescent protein- tagged gonadotropin-releasing hormone neurons in transgenic mice. J Neurosci 1999;19(6):2037–50.
[32] Paxinos G, Watson C. The rat brain in stereotaxic coordinates sixth edition by. Academic press 2006; vol. 170: 547612-.
[33] Czieselsky K, Prescott M, Porteous R, et al. Pulse and surge profiles of luteinizing hormone secretion in the mouse. Endocrinology 2016;157(12):4794–802.
[34] Padilla SL, Qiu J, Soden ME, et al. Agouti-related peptide neural circuits mediate adaptive behaviors in the starved state. Nat Neurosci 2016;19(5):734–41.
[35] Steyn FJ, Wan Y, Clarkson J, Veldhuis JD, Herbison AE, Chen C. Development of a methodology for and assessment of pulsatile luteinizing hormone secretion in juvenile and adult male mice. Endocrinology 2013;154(12):4939–45.
[36] Moore AM, Abbott G, Mair J, Prescott M, Campbell RE. Mapping GABA and glutamate inputs to gonadotropin-releasing hormone (GnRH) neurones in male and female mice. J Neuroendocrinol 2018 Dec;30(12):e12657.
[37] Urban A, Rancillac A, Martinez L, Rossier J. Deciphering the neuronal circuitry controlling local blood flow in the cerebral cortex with Optogenetics in PV::Cre transgenic mice. Front Pharmacol 2012;3:105.
[38] Marshall CJ, Desroziers E, McLennan T, Campbell RE. Defining subpopulations of arcuate nucleus GABA neurons in male, female, and prenatally androgenized female mice. Neuroendocrinology 2017;105(2):157–69.
[39] Campos P, Herbison AE. Optogenetic activation of GnRH neurons reveals minimal requirements for pulsatile luteinizing hormone secretion. Proc Natl Acad Sci U S A 2014;111(51):18387–92.
[40] Han SY, McLennan T, Czieselsky K, Herbison AE. Selective optogenetic activation of arcuate kisspeptin neurons generates pulsatile luteinizing hormone secretion. Proc Natl Acad Sci U S A 2015;112(42):13109–14.
[41] Han SY, Clarkson J, Piet R, Herbison AE. Optical approaches for interrogating neural circuits controlling hormone secretion. Endocrinology 2018;159(11):3822–33.
[42] Clarke IJ, Cummins JT. GnRH pulse frequency determines LH pulse amplitude by altering the amount of releasable LH in the pituitary glands of ewes. J Reprod Fertil 1985;73(2):425–31.
[43] Atasoy D, Betley JN, Su HH, Sternson SM. Deconstruction of a neural circuit for hunger. Nature 2012;488(7410):172–7.
[44] Assaf F, Schiller Y. The antiepileptic and ictogenic effects of optogenetic neurostimulation of PV-expressing interneurons. J Neurophysiol 2016;116(4):1694–704.
[45] Urban A, Rancillac A, Martinez L, Rossier J. Deciphering the neuronal circuitry controlling local blood flow in the cerebral cortex with Optogenetics in PV::Cre transgenic mice. Front Pharmacol 2012;3:105.
[46] Piet R, Kalil B, McLennan T, Porteous R, Czieselsky K, Herbison AE. Dominant neuropeptide Cotransmission in Kisspeptin-GABA regulation of GnRH neuron firing driving ovulation. J Neurosci 2018;38(28):6310–22.
[47] Zuure WA, Roberts AL, Quennell JH, Anderson GM. Leptin signaling in GABA neurons, but not glutamate neurons, is required for reproductive function. J Neurosci 2013;33(45):17874–83.
[48] Chachlaki K, Malone SA, Qualls-Creekmore E, et al. Phenotyping of nNOS neurons in the postnatal and adult female mouse hypothalamus. J Comp Neurol 2017;525(15):3177–89.
[49] Qiu J, Nestor CC, Zhang C, et al. High-frequency stimulation-induced peptide release synchronizes arcuate kisspeptin neurons and excites GnRH neurons. Elife 2016;5.
[50] Zhang X, van den Pol AN. Rapid binge-like eating and body weight gain driven by zona incerta GABA neuron activation. Science 2017;356(6340):853–9.
[51] Wildt L, Hausler A, Marshall G, et al. Frequency and amplitude of gonadotropin-releasing hormone stimulation and gonadotropin secretion in the rhesus monkey. Endocrinology 1981;109(2):376–85.
[52] Roland AV, Moenter SM. Prenatal androgenization of female mice programs an increase in firing activity of gonadotropin-releasing hormone (GnRH) neurons that is reversed by metformin treatment in adulthood. Endocrinology 2011;152(2):618–28.
[53] Zincarelli C, Soltys S, Rengo G, Rabinowitz JE. Analysis of AAV serotypes 1-9 mediated gene expression and tropism in mice after systemic injection. *Molecular therapy : the journal of the American Society of.* Gene Ther 2008;16(6):1073–80.
[54] Hamed SA. The effect of epilepsy and antiepileptic drugs on sexual, reproductive and gonadal health of adults with epilepsy. Expert Rev Clin Pharmacol 2016;9(6):807–19.
[55] Kettel LM, Roseff SJ, Berga SL, Mortola JF, Yen SS. Hypothalamic-pituitary-ovarian response to clomiphene citrate in women with polycystic ovary syndrome. Fertil Steril 1993;59(3):532–8.
[56] Weiss NS, Kostova E, Nahuis M, Mol BWJ, van der Veen F, van Wely M. Gonadotrophins for ovulation induction in women with polycystic ovary syndrome. Cochrane Database Syst Rev 2019;1:CD010290.
[57] Legro RS. Ovulation induction in polycystic ovary syndrome: current options. Best Pract Res Clin Obstet Gynaecol 2016;37:152–9.
[58] Crisosto N, Echiburu B, Maliqueo M, et al. Reproductive and metabolic features during puberty in sons of women with polycystic ovary syndrome. Endocr Connect 2017;6(8):607–13.